11. Structure of the Muonionalusta Iron Meteorite and a Method of Determining the Orientation of Lamellae of Octahedrites.

By

David Malmqvist.

Abstract.

In the present article the lamellar orientation of the Muonionalusta iron meteorite is determined by angle measurements of the lamellar traces on the different faces of ground and etched samples of the meteorite. From this it is found that the lamellae of the meteorite are not orientated parallel to the faces of an octahedron but to the faces of a tetragonal pyramid of a specific character. A method is described whereby it is possible, on a given octahedrite to distinguish between the octahedral structure and the Muonionalusta structure by determining on one plane only the angles between the traces of the lamellae of four lamellar systems. The microstructure of the Muonionalusta iron is described and finally it is discussed if the formation of the structure has been controlled by a tetragonal phase which would separate during slow cooling of the meteoric iron. The axial ratio of the tetragonal pyramid corresponds to that of a tetragonal lattice of the so-called closest tetragonal packing. The tetragonal cell appears to be a transitional form between the cell of the cubic face-centred γ-phase and the cell of the cubic body-centred α-phase of iron-nickel.

Introduction.

Sixteen years ago Professor H. BACKLUND suggested that the author should carry out an investigation on the Muonionalusta iron meteorite, most of the material of which belongs to the meteorite collection at the Mineralogical Geological Institution of Upsala. The results of these structure studies were read before the Swedish Mineralogical Society in a lecture on Dec. 11th, 1931. It was intended to publish the results at that time but much intervening work has prevented the author from so doing.

In the summer of 1946 the Muonionalusta meteorite was again brought into actuality by the discovery of a new iron meteorite at Kitkiöjoki not far

from the finding place of the Muonionalusta meteorite. This new meteorite was reported by N. ZENZÉN (1) who called it Muonionalusta II. In connection with this new discovery some method of identification must be evolved if one proposes to solve the problem: Do the two meteorites belong to the same fall or not? For this reason the author has found it better to publish the present paper although the research has not been brought to the stage that was originally intended. This is done in the hope that *inter alia* the new viewpoints may contribute to solve the above-mentioned problem.

Even at a very early stage of the investigation it was evident that the kamacite (taenite) lamellae of the Muonionalusta meteorite were not orientated parallel to the faces of an octahedron, as they generally are assumed to be in octahedrites of the same class. As regards this discrepancy, nothing has been reported previously concerning it as the author was of the opinion that this fact had not been proved satisfactorily. From a recent recalculation of the measurements obtained in 1931 the author obtained exactly the same results as before and the statement can thus be considered conclusive. Most of the present article is taken up by questions connected with the orientation of lamellae, since it seems to throw some new light not only on iron meteorite problems in general but also on problems which are concerned with the equilibrium diagram of technical iron-nickel.

Concerning the circumstances connected with the discovery, the shape, the mineralogical composition, etc. of the Muonionalusta meteorite the reader is referred to the excellent description by A. G. HÖGBOM (2), in whose paper all the essential facts are included. To this description the author has very little to add. Only in some details concerning the structures does the author have a somewhat different opinion. The differences of opinion depend mostly on the fact that this investigation has been carried out with the aid of a metallographic microscope whereby the structural constituents can be studied in a much more convenient manner. On the whole this article may be considered as a complement to the description by HÖGBOM.

CHAPTER I.

Determination of lamellar orientation.

a) Technique of the determination.

The determinations described in this article were made on two small samples cut from a larger sample (weight 306 gr) which formerly was included in a collection belonging to HJALMAR LUNDBOHM and which after his death was returned to the meteorite collection at the Mineralogical Geological Institution. LUNDBOHM's sample was cut from the Muonionalusta iron in 1910 in connection with the research made by HÖGBOM at that time. The larger sample, sample 1, of the two samples which were determined was cut

from LUNDBOHM's sample in the shape of a rectangular prism of which faces b_1, c_1 and f_1 were ground plane. Faces c_1 and f_1 are nearly parallel. The prism is cut almost perpendicularly by a fourth face d_1 and somewhat obliquely by a fifth face e_1. The smaller sample, sample 2, was cut in the form of a triangular prism with faces b_2, d_2 and e_2. The prism is cut obliquely by a fourth face c_2.

Sample 1 has a weight of 14.4 gr, a length of about 2.1 cm, a breadth of 1.6 cm and a height of 0.7 cm. Sample 2 has a weight of 3.3 gr, a length of about 1.7 cm, a breadth of 0.8 cm and a height of 0.6 cm.

The faces of the samples were ground very carefully and then polished in order to give perfect reflexes for the goniometric measurements. The interfacial angles were determined with an one-circle goniometer. According to the usual method for this kind of determination the edge between two faces was adjusted to be parallel to the rotation axis of the goniometer. By steps the angles between pairs of adjacent faces were determined in this manner and from the measurement values the relative position of all the faces can be calculated.

Thereafter, the sample was etched for 10 minutes in dilute HNO_3, washed with distilled water and alcohol and finally air dried.

The sample was then mounted in the usual way on an object-glass, which was placed on the revolving table of a metallographic microscope. On every face the angles between the face-edges and the traces of the different lamellae of the surfaces were determined. This was done by translating the sample parallel and then rotating it until an edge or a lamellar trace coincided with the hair cross in the eyepiece. At every coincidence the reading on the angular scale of the revolving table was recorded. The angle measurements of a given lamellar system were not executed on one lamella of the system only, but in order to obtain an idea of the measurement errors, four or five lamellae or as many lamellae of the system as could be seen on the surface under examination were measured.

b) Determinations on sample 1.

In Fig. 1, sample 1 is assumed to be opened out flat along the edges $[b_1\ d_1]$[1] and $[b_1\ e_1]$ and drawn in one plane. If one desires to make a model of the sample, make a copy of the figure and cut away the blank triangular-shaped parts lying next to the prepared faces of the figure with a pair of scissors. Thereafter fold the paper along the edges and gum together edges $[b_1\ d_1]$ and $[b_1\ e_1]$. In this way a comprehensible figure of the spatial arrangement is obtained not only of the prepared faces but also of the lamellar systems. The lamellar directions of a certain system lie, as may be seen, in one plane.

[1] In the following text the edge between two sample faces, e. g. b_1 and d_1 is denoted as $[b_1\ d_1]$. The lamellae are denoted as I, II, III, IV and the edge between say b_1 and I, i. e., the trace of lamella I on the face b_1, is denoted $[b_1$ I].

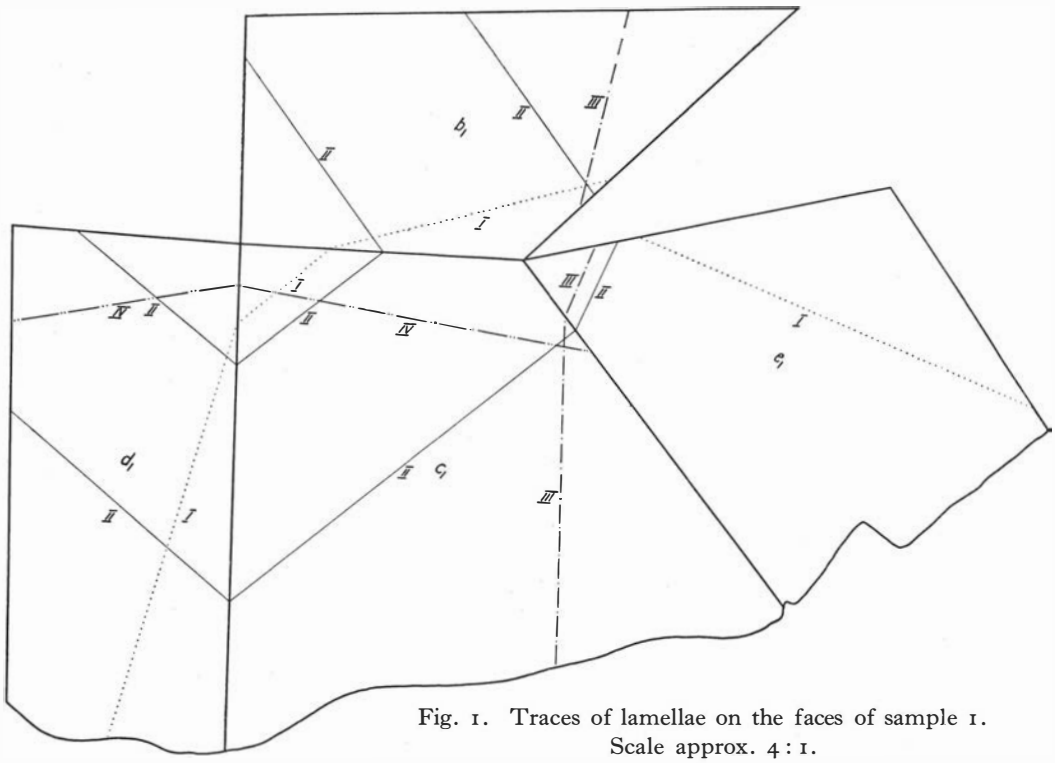

Fig. 1. Traces of lamellae on the faces of sample 1. Scale approx. 4 : 1.

If we consider the lamellae as crystal faces and the traces of the lamellae on a certain section as edges between two crystal faces we can, with only a few modifications, calculate the relative positions of the lamallae according to those laws which apply to ordinary crystallographic calculations. From the goniometer measurements (Table I) the positions of the prepared faces are known and from the angle measurements with the metallographic microscope the angles between the edges and the traces of the lamellae are known (Table II). Obviously the precision obtained by this method of determination

Table I. Goniometric measurements of the samples 1 and 2.

Sample 1					Sample 2				
Faces		Reflex on 1st face	Reflex on 2nd face	Inter-facial angle	Faces		Reflex on 1st face	Reflex on 2nd face	Inter-facial angle
b_1	e_1	205° 5′	263° 4′	57° 59′	b_2	c_2	145° 32′	232° 26′	86° 54′
c_1	b_1	132 3	219 1	86 58	b_2	e_2	253 31	122 49	130 42
c_1	d_1	194 45	282 14	87 29	c_2	e_2	164 21	286 38	122 17
c_1	e_1	290 20	239 6	51 14	c_2	d_2	186 54	259 56	73 2
d_1	b_1	171 34	262 56	91 22	e_2	d_2	123 1	38 45	84 16

Table II. Measurements of angles between the edges on sample 1.

Edges	Readings. Mean values	Number of readings	Mean errors for one observ.	Angle between edges	Angle between edges. Measured	Angle between edges. Calculated	Remarks
$[b_1 c_1]$	43.9°	4	±0.1°	$[b_1 e_1] \wedge [b_1 c_1]$	45.4°	45° 4′	
$[b_1 e_1]$	89.3	3	0.0				
$[b_1 d_1]$	(318.2)	2	2.2				Edge somewhat rounded
$[b_1$ I]	60.2	4	0.6	$[b_1 c_1]$ $[b_1$ I]	16.3		
$[b_1$ III]	124.0	3	0.5	$[b_1 c_1]$ $[b_1$ III]	80.1		
$[b_1$ II]	174.8	3	0.4	$[b_1 c_1]$ $[b_1$ II]	130.9		
$[c_1 e_1]$	320.6	7	0.3	$[c_1 e_1]$ $[c_1 b_1]$	50.5	50 20	
$[c_1 b_1]$	11.1	6	0.3	$[c_1 d_1]$ $[c_1 b_1]$	91.4	91 30	
$[c_1 d_1]$	102.5	5	0.1				
$[c_1$ II]	232.8	12	0.5	$[c_1 b_1]$ $[c_1$ II]	41.7		
$[c_1$ I]	235.0	3	0.3	$[c_1 b_1]$ $[c_1$ I]	43.9		
$[c_1$ III]	103.1	7	0.6	$[c_1 b_1]$ $[c_1$ III]	92.0		
$[c_1$ IV]	183.6	9	0.5	$[c_1 b_1]$ $[c_1$ IV]	172.5		
$[d_1 b_1]$	311.4	4	0.1	$[d_1 b_1]$ $[d_1 c_1]$	93.0	93 6	
$[d_1 c_1]$	44.4	4	0.2				
$[d_1$ II]	275.7	7	0.6	$[d_1 c_1]$ $[d_1$ II]	51.3		
$[d_1$ IV]	325.0	5	0.3	$[d_1 c_1]$ $[d_1$ IV]	100.6		
$[d_1$ I]	28.5	7	0.7	$[d_1 c_1]$ $[d_1$ I]	164.1		
$[e_1 c_1]$	130.5	5	0.2	$[e_1 c_1]$ $[e_1 b_1]$	65.0	65 3	
$[e_1 b_1]$	195.6	4	0.2				
$[e_1$ II]	248.6	5	0.2	$[e_1 c_1]$ $[e_1$ II]	118.1		
$[e_1$ III]	251.4	4	0.3	$[e_1 c_1]$ $[e_1$ III]	120.9		
$[e_1$ I]	340.5	2	0.6	$[e_1 c_1]$ $[e_1$ I]	30.0		

of lamellar positions cannot be the same as that with which we are familiar in ordinary crystallographic measurements where, if the face-reflexes are satisfactory, the calculations are based on very exact angle determinations. Therefore the claims on accuracy must be less exacting.

If we indicate the interfacial angle between two prepared faces (for instance c_1 and b_1, see Fig. 2) by R, the interfacial angle between a prepared face c_1 and a lamella (for instance lamella II) by S, the angle between the zoneplanes $c_1\ b_1$ and c_1 II (i. e., the same angle as between the edge $[c_1\ b_1]$ and the trace of the lamella II on the face c_1) by τ and the angle between the zoneplanes $b_1\ c_1$ and b_1 II (i. e., the same angle as between the edge $[c_1\ b_1]$ and the trace of the lamella II on the face b_1) by σ, we obtain, according to the cotangent-theorem of spherical trigonometry, the following relation

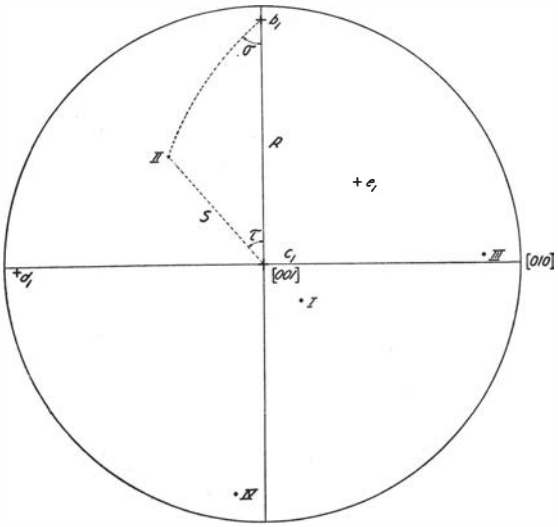

Fig. 2. Stereographic projection of faces and lamellae of sample 1.

$$\cot S \sin R = \cos R \cos \tau + \sin \tau \cot \sigma, \tag{1}$$

which for numerical calculations can be transformed into the more practical form

$$\cot S = \frac{\cot R \sin (\tau + \psi)}{\sin \psi} \tag{2 a}$$

and

$$\tan \psi = \cos R \tan \sigma \tag{2 b}$$

where

$$\psi = \text{a fictitious angle.}$$

As shown from the stereographic projection of sample 1 in Fig. 2, the c-axis [001] is chosen to lie perpendicularly to face c_1 and the zoneplane $c_1\ b_1$ to lie perpendicularly to the b-axis [010]. With this arrangement we can, with the aid of formulae (2 a) and (2 b), calculate the positions of the lamellae which according to convention are denoted in spherical coordinates, i. e., the polar distance ϱ (0—90°) from the c-axis and the azimuth φ from the b-axis where the angles are measured clock-wise from 0° to 360°. Accordingly we have $\varrho = S$ and $\varphi = 270° - \tau$.

From the angle determinations of Tables I and II we obtain, in Table III, the calculated coordinates of the lamellae I, II, III and IV applicable to the above-mentioned coordinate system. As is shown in Table III, the coordinates represent mean values, generally from two different calculations. As shown by the formulae the angle determinations on two faces are obviously sufficient to calculate the coordinates of a lamellar system. The two faces

Table III. Lamellar positions of samples 1 and 2.

Sample 1						Sample 2					
Lamellar system	Angle determ. on faces	φ	ϱ	Mean values φ	Mean values ϱ	Lamellar system	Angle determ. on faces	φ	ϱ	Mean values φ	Mean values ϱ
I	c_1 e_1	46.1°	23.6°			I	c_2 b_2	46.8°	22.3°		
	c_1 b_1	»	22.8				c_2 e_2	»	24.4		
				46.1°	23.2°					46.8°	23.4°
II	c_1 e_1	228.3	55.8			II	c_2 b_2	223.5	57.2		
	c_1 b_1	»	58.3				c_2 e_2	»	57.8		
	c_1 d_1	»	57.3							223.5	57.5
				228.3	57.1	III	c_2 e_2	93.0	78.5		
III	c_1 e_1	358.0	80.7							93.0	78.5
	c_1 b_1	»	80.0			IV	c_2 b_2	354.3	80.0		
				358.0	80.3		c_2 e_2	»	80.7		
IV	c_1 e_1	97.5	79.1							354.3	80.4
				97.5	79.1						

on which angle determinations have been performed in order to calculate the position of a given lamellar system are denoted in a special column in Table III. If varying coordinate values have been recorded for a certain lamellar system the arithmetic mean of the coordinates has been calculated and considered as the most probable one.

c) Determinations on sample 2.

In Fig. 3, sample 2 is drawn in one plane in the same way as described above. Fig. 4 shows the position of the faces and of the different lamellar systems in stereographic projection. The calculation of the lamellar positions is carried out in identically the same manner as already described and the angle determinations on which the calculations are based appear in Tables I and IV. The results of the calculations appear in Table III.

As seen from Tables III and IV, the accuracy of the angle measurements of this sample is not as great as that of sample 1. This is due to the less perfect edges which had been somewhat rounded during grinding and polishing. However the results of the measurements of sample 2 are included because they verify the results from sample 1.

Face d_2 was not measured since it was very difficult to distinguish between the four lamellar systems, pairs of which formed groups whose members were nearly parallel to each other. As will be seen later, the face represents a section nearly perpendicular to the c-axis if the iron is orientated in a sym-

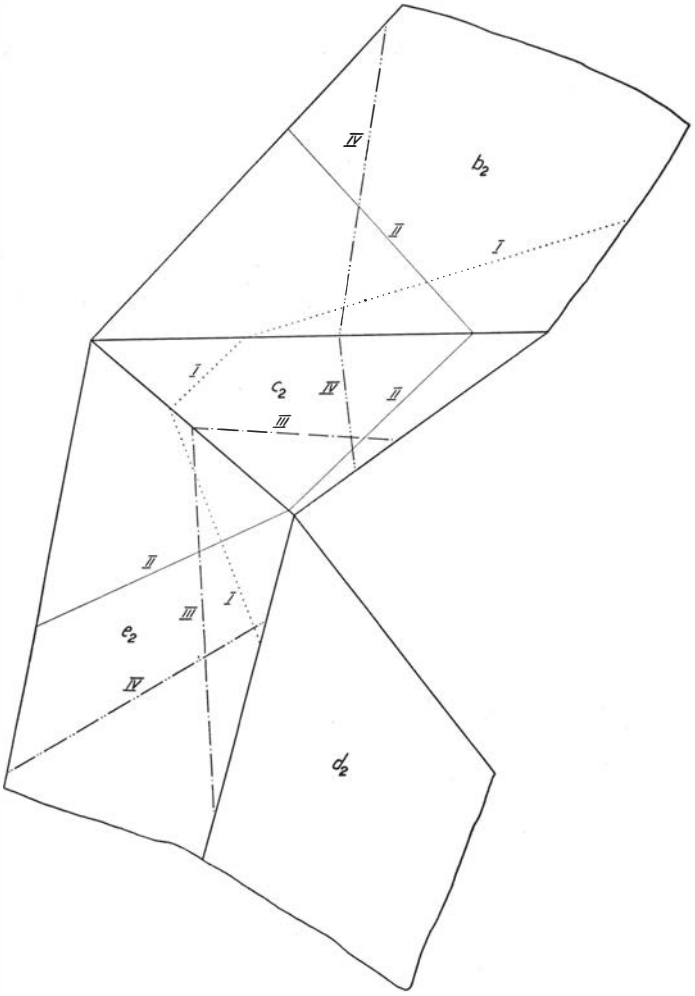

Fig. 3. Traces of lamellae on the faces of sample 2.
Scale approx. 4 : 1.

metrical position in relation to the lamellar systems. In addition the two lamellar systems I and II nearly coincide on the c_2-face but they are distinguishable from one another due to a pronounced difference in breadth. From Table IV it is evident that the lamellar systems III and IV have been numbered in a different manner on samples 1 and 2. They have obviously been interchanged. This fact however, has no influence on the following calculations.

d) Calculation of interlamellar angles.

From a knowledge of the position of the lamellae the interlamellar angles can easily be deduced. According to the law of cosines for sides we have:—

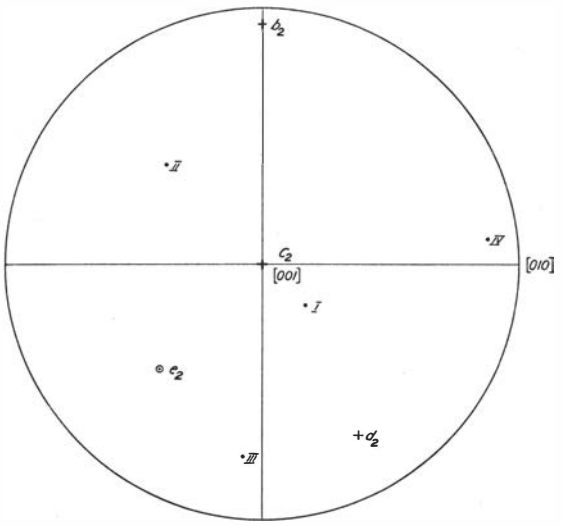

Fig. 4. Stereographic projection of faces and lamellae of sample 2.

$$\cos I_{1,2} = \cos \varrho_1 \cos \varrho_2 + \sin \varrho_1 \sin \varrho_2 \cos (\varphi_2 - \varphi_1), \qquad (3)$$

where

$I_{1,2}$ = the interfacial angle between two lamellar systems (for instance lamellae I and II)

ϱ_1 = » polar distance of the one lamellar system (for instance lamella I)

ϱ_2 = » » » » » other lamellar system (for instance lamella II)

φ_1 = » azimuth of the one lamellar system (for instance lamella I)

φ_2 = » » » » other lamellar system (for instance lamella II).

By means of formula (3) we can calculate the interlamellar angle between any two lamellar systems (for instance as in the formula above the lamellar combination I, II or I, III; I, IV etc.) and the results of this calculation are shown in Table V. In this Table we can distinguish between two groups of interlamellar angles one group of which includes angles about 81° (supplementary angles 99°), and the other group angles about 65° (supplementary angles 115°). *Thus it is evident that the interlamellar angles of the Muonionalusta iron meteorite are not the same as the interlamellar angles of a true octahedrite* (70.5°). The divergences are much too great to be explained by errors of measurement in the angle determinations, for if explained in such a way the deviations should lie well outside the error limits.

Table IV. Measurements of angles between the edges on sample 2.

Edges	Readings. Mean values	Number of readings	Mean errors for one observ.	Angle between edges	Angle between edges. Measured	Angle between edges. Calculated	Remarks
$[b_2\,c_2]$	2.8°	3	±0.5°				
$[b_2\,e_2]$	49.2	5	0.5	$[b_2\,c_2] \wedge [b_2\,e_2]$	46.4°	48° 47′	
$[b_2\,\mathrm{I}]$	18.3	6	0.7	$[b_2\,c_2]$ $[b_2\,\mathrm{I}]$	15.5		
$[b_2\,\mathrm{IV}]$	263.1	5	0.6	$[b_2\,c_2]$ $[b_2\,\mathrm{IV}]$	80.3		
$[b_2\,\mathrm{II}]$	314.3	4	0.8	$[b_2\,c_2]$ $[b_2\,\mathrm{II}]$	131.5		Only 3 lamellae
$[c_2\,b_2]$	293.5	2	0.2				
$[c_2\,e_2]$	72.3	3	0.1	$[c_2\,b_2]$ $[c_2\,e_2]$	41.2	42 25	
$[c_2\,d_2]$	(147.8)	2	2.8				Edge very rounded
$[c_2\,\mathrm{I}]$	336.7	4	0.4	$[c_2\,b_2]$ $[c_2\,\mathrm{I}]$	43.2		
$[c_2\,\mathrm{II}]$	336.8	4	0.2	$[c_2\,b_2]$ $[c_2\,\mathrm{II}]$	43.3		Lamellar systems I and II nearly coinciding
$[c_2\,\mathrm{IV}]$	29.2	5	0.4	$[c_2\,b_2]$ $[c_2\,\mathrm{IV}]$	84.3		
$[c_2\,\mathrm{III}]$	110.5	4	0.5	$[c_2\,b_2]$ $[c_2\,\mathrm{III}]$	177.0		
$[e_2\,b_2]$	54.9	4	0.1				
$[e_2\,c_2]$	116.2	3	0.2	$[e_2\,b_2]$ $[e_2\,c_2]$	61.3	62 41	
$[e_2\,d_2]$	50.5	4	0.2	$[e_2\,d_2]$ $[e_2\,c_2]$	65.7	64 53	Edge somewhat rounded
$[e_2\,\mathrm{II}]$	181.0	5	0.2	$[e_2\,c_2]$ $[e_2\,\mathrm{II}]$	64.8		
$[e_2\,\mathrm{IV}]$	185.9	5	0.3	$[e_2\,c_2]$ $[e_2\,\mathrm{IV}]$	69.7		
$[e_2\,\mathrm{III}]$	249.7	4	1.0	$[e_2\,c_2]$ $[e_2\,\mathrm{I}]$	133.5		Only 2 lamellae
$[e_2\,\mathrm{I}]$	267.4	6	0.4	$[e_2\,c_2]$ $[e_2\,\mathrm{III}]$	151.2		

e) Lamellar orientation.

From the calculated values of the interlamellar angles of Table V we can determine the relative lamellar positions. On plotting the results in a stereographic projection we obtain the lamellar positions shown in Fig. 5. In order to determine the symmetry, we must calculate the angles, which are denoted by bars above their numerical values. As seen in Fig. 5, the angle between the zoneplanes I—II and III—IV is found by calculation to be exactly 90.0°. Hence, it is convenient to perform a coordinate displacement, making the *c*-axis parallel to the line of intersection between the zoneplanes I—II and III—IV. In this manner we obtain the lamellar projections of Fig. 6 where the above-mentioned zoneplanes are drawn 45° from the axis

Table V. Interlamellar angles of the Muonionalusta meteorite.

	Lamellae	Group I. Angle	Group II. Angle	Group I. Supplementary angle	Group II. Supplementary angle	Group I.	Group II.
Sample 1	I : II	80.3°				80.3°	
	I : III		65.5°				65.5°
	I : IV		65.5				65.5
	II : III				115.9°		64.1
	II : IV				115.8		64.2
	III : IV			97.4°		82.6	
Sample 2	I : II	81.1				81.1	
	I : III		64.8				64.8
	I : IV		66.9				66.9
	II : III				112.6		67.4
	II : IV				117.3		62.7
	III : IV			100.5		79.5	

Mean values: 80.9° ± 0.7° 65.1° ± 0.6°

planes *ac* and *bc*. This is also done in order to demonstrate the difference between the lamellar positions I, II, III, IV of the Muonionalusta meteorite and those of a true octahedrite whose poles are indicated by small squares in Fig. 6. Moreover, in Fig. 6 the poles of all the faces of samples 1 and 2 are plotted as well as the pole of the polished section which appears in Fig. 3 of HÖGBOM's paper (hereafter denoted as Section *H.* or *S. H.*). How the position of this section is determined will be reported in the next chapter.

From the axial position chosen in Fig. 6 it is easy to see that the *c*-axis represents a four-fold axis of symmetry. However, the *a*- and *b*-axes are not, as in the cubic system, four-fold axes of symmetry but two-fold ones. Therefore we must draw the conclusion that *the Wiedmannstätten figures of the Muonionalusta iron meteorite are not orientated parallel to the faces of an octahedron but to the faces of a tetragonal pyramid.* The lamellae lie at a more obtuse angle to the *c*-axis than the octahedral planes. Since $\cot 49.5° = 0.853 \simeq \frac{\sqrt{3}}{2}$, the axial ratio is found to be

$$a : c = 1 : \frac{\sqrt{2}}{2 \cdot 0.853} = 1 : 0.829 \simeq 1 : \sqrt{\frac{2}{3}}.$$

Indeed, the above-mentioned conclusion is somewhat remarkable. Many unsolved questions arise in connection with this statement. Does the

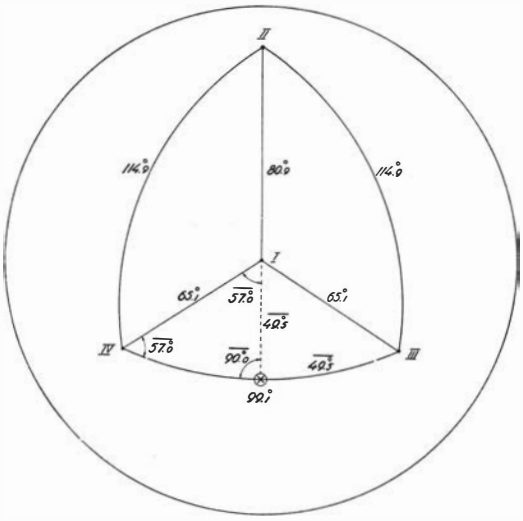

Fig. 5. Stereographic projection showing interlamellar angles and angles between zone planes.

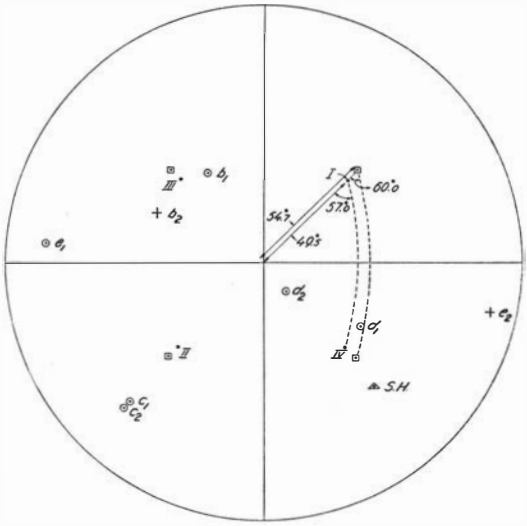

+ (upper half) } poles of the faces of samples 1 and 2.
⊙ (lower half) }
• of the lamellae I, II, III and IV of the Muonionalusta iron meteorite.
△ of section *H* (*S. H.*).
▣ of the lamellae of a true octahedrite.

Fig. 6.

Muonionalusta iron meteorite represent a new type of iron meteorite or not? Is it a common or a rare type or do most of the so-called octahedral iron meteorites belong to same type? Are the WIEDMANNSTÄTTEN figures mostly orientated parallel to the octahedral faces in octahedral iron or has it often only been assumed that they are? Does the Muonionalusta type represent a fixed type of iron meteorite or do other transitional forms of tetragonal symmetry exist? Naturally all these questions cannot be answered unless a systematic investigation of several iron meteorites is carried out. The author's opinion is that we know little about this subject. However, the questions may at any rate be of importance for the classification of iron meteorites.

CHAPTER II.

A method of determining the type of octahedrites and the position of sections.

a) Application of the method.

In order to determine the type of a given octahedrite[1] the author has elaborated an improved method which is not as laborious as that described in chapter I. According to this new method it is in general possible from angle determinations on only one given section to decide whether the octahedrite belongs to the true octahedral type ("octahedron" type), to the Muonionalusta type or to neither. If belonging to either of these two types, it is possible to determine simultaneously the position of the section relative to the lamellar systems. An advantage of the method is further that it permits the necessary determinations being made on existing photographs or micrographs of etched sections of iron meteorites. In the method the determinations require the presence of a section in which all the lamellar systems are visible. Unfortunately photographs of just such a section seem to be rather uncommon in the meteorite literature, probably because they are not considered representative. Besides, it is difficult to take a micrograph in which four lamellar systems are visible.

Similar methods for determining the orientation of octahedrites have formerly been elaborated by A. HIMMELBAUER (3), J. LEONHARDT (4) and others. The older methods are mostly graphic (stereographic projection methods) and are not exact enough to be used in this connection. Neither can the more exact method of LEONHARDT be used directly as its application is possible only when an octahedral orientation is postulated.

[1] The term "octahedrite" is, though illogically, also used for the Muonionalusta type.

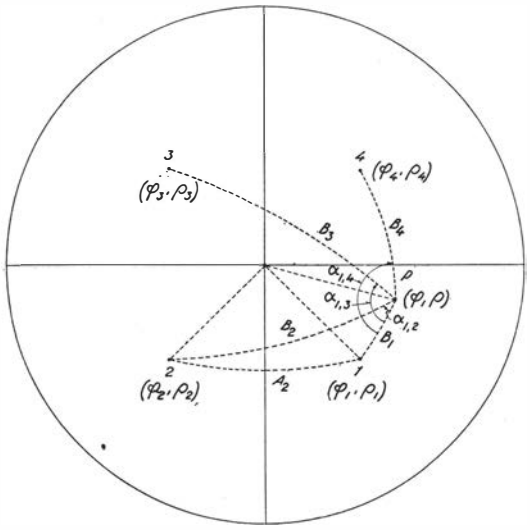

Fig. 7.

b) Deduction of formulae.

If we propose to calculate the angle differences between the traces of the four lamellar systems on a certain section we can do so in the following manner. We suppose that pole P (see Fig. 7) has the coordinates (φ, ϱ) and the poles of the lamellae 1, 2, 3, 4 in the quadrants 1, 2, 3, 4 of the upper half of the projection sphere have the coordinates (φ_1, ϱ_1), (φ_2, ϱ_2), (φ_3, ϱ_3) and (φ_4, ϱ_4) respectively. Let the angle between the traces of lamellae 1 and 2 be denoted by $\alpha_{1,2}$, between lamellae 1 and 3 by $\alpha_{1,3}$ and between lamellae 1 and 4 by $\alpha_{1,4}$. Assume that pole P lies in the 1st quadrant. Since there exist a four-fold axis of symmetry and a centre of symmetry the problem is identical in all four quadrants as well in the upper as in the lower part of the projection sphere. Hence we can put the coordinates of P inside the limits

$$0^\circ \leqq \varphi \leqq 90^\circ$$
$$0^\circ \leqq \varrho \leqq 90^\circ.$$

Let angles $\alpha_{1,2}$, $\alpha_{1,3}$ and $\alpha_{1,4}$ be measured clockwise from the trace of lamella 1 in the same quadrant as the pole of the section (quadrant 1).

Finally, the interfacial angles (the lamellae are still regarded as faces) between P and lamellae 1, 2, 3 and 4 are denoted by B_1, B_2, B_3 and B_4 respectively and the interfacial angles between lamella 1 and lamellae 2, 3 and 4 by A_2, A_3 and A_4 respectively.

Let $\varrho_1 = \varrho_2 = \varrho_3 = \varrho_4$ then, according to the law of cosines for sides, we obtain the following equations:—

$$\cos B_{1-4} = \cos \varrho \cos \varrho_1 + \sin \varrho \sin \varrho_1 \cos (\varphi_{1-4} - \varphi), \tag{4}$$

$$\cos A_{2-4} = \cos^2 \varrho_1 + \sin^2 \varrho_1 \cos (\varphi_{2-4} - \varphi_1), \tag{5}$$

$$\cos A_{2-4} = \cos B_1 \cos B_{2-4} + \sin B_1 \sin B_{2-4} \cos \alpha_{1,2-4}. \tag{6}$$

As may be easily understood, equation (4) covers four equations while equations (5) and (6) cover three each.

Due to the symmetry $\varphi_1 = 45^\circ$, $\varphi_2 = 135^\circ$, $\varphi_3 = 225^\circ$ and $\varphi_4 = 315^\circ$, $\varphi_2 - \varphi_1 = 90^\circ$, $\varphi_3 - \varphi_1 = 180^\circ$ and $\varphi_4 - \varphi_1 = 270^\circ$.

α) *The octahedron case:*

In an octahedron the angle $\varrho_1 = 54^\circ 44'$ and thus

$$\cos \varrho_1 = \frac{\sqrt{3}}{3} \text{ and } \sin \varrho_1 = \sqrt{\frac{2}{3}}.$$

Hence, we obtain from equations (4)

$$\cos B_1 = \frac{\sqrt{3}}{3} [\cos \varrho + \sin \varrho (\cos \varphi + \sin \varphi)] = \frac{\sqrt{3}}{3} C_1, \tag{7}$$

$$\cos B_2 = \frac{\sqrt{3}}{3} [\cos \varrho - \sin \varrho (\cos \varphi - \sin \varphi)] = \frac{\sqrt{3}}{3} C_2, \tag{8}$$

$$\cos B_3 = \frac{\sqrt{3}}{3} [\cos \varrho - \sin \varrho (\cos \varphi + \sin \varphi)] = \frac{\sqrt{3}}{3} C_3, \tag{9}$$

$$\cos B_4 = \frac{\sqrt{3}}{3} [\cos \varrho + \sin \varrho (\cos \varphi - \sin \varphi)] = \frac{\sqrt{3}}{3} C_4, \tag{10}$$

and from equations (5)

$$\cos A_2 = \cos A_4 = \tfrac{1}{3}, \tag{11}$$

$$\cos A_3 = -\tfrac{1}{3} \tag{12}$$

which gives, according to equations (6)

$$\cos \alpha_{1,2} = \frac{1 - C_1 C_2}{[(3 - C_1^2)(3 - C_2^2)]^{\frac{1}{2}}}, \tag{13}$$

$$\cos \alpha_{1,3} = -\frac{1 + C_1 C_3}{[(3 - C_1^2)(3 - C_3^2)]^{\frac{1}{2}}}, \tag{14}$$

$$\cos \alpha_{1,4} = \frac{1 - C_1 C_4}{[(3 - C_1^2)(3 - C_4^2)]^{\frac{1}{2}}}, \tag{15}$$

where

$$C_1 = \cos \varrho + \sin \varrho (\cos \varphi + \sin \varphi),$$
$$C_2 = \cos \varrho - \sin \varrho (\cos \varphi - \sin \varphi),$$
$$C_3 = \cos \varrho - \sin \varrho (\cos \varphi + \sin \varphi),$$
$$C_4 = \cos \varrho + \sin \varrho (\cos \varphi - \sin \varphi).$$

A Table of angles at the end of this article shows the result of a computation, using the formulae above, of the α-values for some given values of φ and ϱ. From the values in the Table the diagram 1 (at the end of the article) was drawn. In order to draw the curves correctly it is important to know the points on the curves at which 1) $\cos\alpha = 0$ ($\alpha = 90° = 270°$) and 2) $\cos\alpha = \pm 1$ ($\alpha = 0°$ and $\alpha = 180°$).

They are

$$1)\quad \cos\alpha_{1,2} = 0, \quad \text{when} \quad \cot\varrho = \frac{\cos^2\varphi}{\sin\varphi},$$

$$\cos\alpha_{1,3} = 0, \quad \text{»} \quad \cot\varrho = (\sin\varphi\cos\varphi)^{\frac{1}{2}},$$

$$\cos\alpha_{1,4} = 0, \quad \text{»} \quad \cot\varrho = \frac{\sin^2\varphi}{\cos\varphi},$$

$$2)\quad \cos\alpha_{1,2} = \pm 1, \quad \text{when} \quad \cos\varrho = \frac{\sin\varphi}{(1+\sin^2\varphi)^{\frac{1}{2}}},$$

$$\cos\alpha_{1,3} = \pm 1, \quad \text{»} \quad \varrho = 0°,$$

$$\cos\alpha_{1,4} = \pm 1, \quad \text{»} \quad \cos\varrho = \frac{\cos\varphi}{(1+\cos^2\varphi)^{\frac{1}{2}}}.$$

As may be seen, the curves of diagram 1 are symmetrical around $\alpha = 180°$ and it would therefore have been possible to draw a diagram where α varied only from 0—180°. Such a diagram however, is not very lucid as will be evident on further consideration.

β) *The Muonionalusta case:*

From the calculation of the axial ratio of the Muonionalusta type we observed that the axial ratio was approximately $1 : \sqrt{\frac{2}{3}}$ and the ϱ_1-value 49.5°. This fact must have a theoretical significance connected with the lattice and will be discussed in more detail in a following chapter. To begin with we shall only use the observation to simplify the formulae below. Thus we have $\cos\varrho_1 = \sqrt{\frac{3}{7}}$ and $\sin\varrho_1 = \sqrt{\frac{4}{7}}$. After identical deductions employed in the treatment of the octahedron case, we obtain from equations (4)

$$\cos B_1 = \sqrt{\frac{3}{7}}\left[\cos\varrho + \sqrt{\frac{2}{3}}\sin\varrho\,(\cos\varphi + \sin\varphi)\right] = \sqrt{\frac{3}{7}}\,C_1, \qquad (16)$$

$$\cos B_2 = \sqrt{\frac{3}{7}}\left[\cos\varrho - \sqrt{\frac{2}{3}}\sin\varrho\,(\cos\varphi - \sin\varphi)\right] = \sqrt{\frac{3}{7}}\,C_2, \qquad (17)$$

$$\cos B_3 = \sqrt{\frac{3}{7}}\left[\cos\varrho - \sqrt{\frac{2}{3}}\sin\varrho\,(\cos\varphi + \sin\varphi)\right] = \sqrt{\frac{3}{7}}C_3, \qquad (18)$$

$$\cos B_4 = \sqrt{\frac{3}{7}}\left[\cos\varrho + \sqrt{\frac{2}{3}}\sin\varrho\,(\cos\varphi - \sin\varphi)\right] = \sqrt{\frac{3}{7}}C_4, \qquad (19)$$

and from equations (5)

$$\cos A_2 = \cos A_4 = \tfrac{3}{7}, \qquad (20)$$

$$\cos A_3 = -\tfrac{1}{7} \qquad (21)$$

which give, according to equations (6)

$$\cos\alpha_{1,2} = \frac{1 - C_1 C_2}{[(\frac{7}{3} - C_1^2)(\frac{7}{3} - C_2^2)]^{\frac{1}{2}}}, \qquad (22)$$

$$\cos\alpha_{1,3} = -\frac{\frac{1}{3} + C_1 C_3}{[(\frac{7}{3} - C_1^2)(\frac{7}{3} - C_3^2)]^{\frac{1}{2}}}, \qquad (23)$$

$$\cos\alpha_{1,4} = \frac{1 - C_1 C_4}{[(\frac{7}{3} - C_1^2)(\frac{7}{3} - C_4^2)]^{\frac{1}{2}}}, \qquad (24)$$

where

$$C_1 = \cos\varrho + \sqrt{\frac{2}{3}}\sin\varrho\,(\cos\varphi + \sin\varphi),$$

$$C_2 = \cos\varrho - \sqrt{\frac{2}{3}}\sin\varrho\,(\cos\varphi - \sin\varphi),$$

$$C_3 = \cos\varrho - \sqrt{\frac{2}{3}}\sin\varrho\,(\cos\varphi + \sin\varphi),$$

$$C_4 = \cos\varrho + \sqrt{\frac{2}{3}}\sin\varrho\,(\cos\varphi - \sin\varphi).$$

Finally $\cos\alpha = 0$ and $\cos\alpha = \pm 1$ respectively at the following points on the curves

1) $\cos\alpha_{1,2} = 0$, when $\cot\varrho = \dfrac{1}{\sin\varphi}\left(\dfrac{1}{2\sqrt{6}} + \sqrt{\dfrac{2}{3}}\cos^2\varphi\right)$,

$\cos\alpha_{1,3} = 0$, » $\cot\varrho = (\frac{1}{4} + \sin\varphi\cos\varphi)^{\frac{1}{2}}$,

$\cos\alpha_{1,4} = 0$, » $\cot\varrho = \dfrac{1}{\cos\varphi}\left(\dfrac{1}{2\sqrt{6}} + \sqrt{\dfrac{2}{3}}\sin^2\varphi\right)$,

2) $\cos\alpha_{1,2} = \pm 1$, when $\cos\varrho = \dfrac{\sin\varphi}{(\frac{2}{3} + \sin^2\varphi)^{\frac{1}{2}}}$,

$\cos\alpha_{1,3} = \pm 1$, » $\varrho = 0^\circ$,

$\cos\alpha_{1,4} = \pm 1$, » $\cos\varrho = \dfrac{\cos\varphi}{(\frac{2}{3} + \cos^2\varphi)^{\frac{1}{2}}}$.

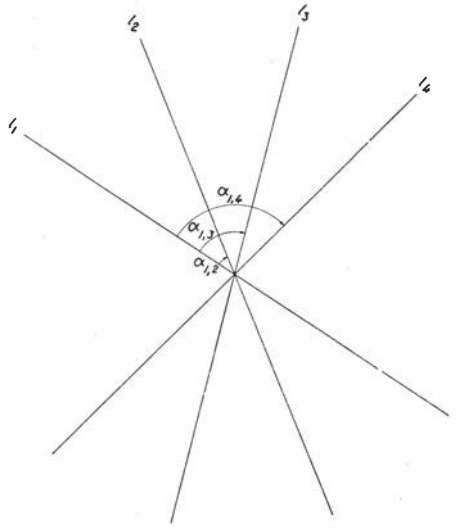

Fig. 8 a. Angles between the traces of the lamellae. The figure shows a possible angle combination if l_1 lies in the 1st, l_2 in the 2nd, l_3 in the 3rd and l_4 in the 4th quadrant.

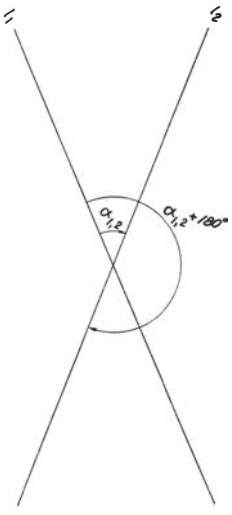

Fig. 8 b. Two possible angles between the traces of the lamellae if l_1 lies in the 1st and l_2 in the 2nd quadrant.

The values in the Table of angles at the end of the article are calculated according to the formulae for the Muonionalusta case. From the Table the curves of diagram 2 are drawn. As may be easily understood the curves of diagram 2 are also symmetrical around $\alpha = 180°$.

c) Directions how to use the diagrams.

Suppose that on a certain section of an octahedrite we observe four lamellar systems denoted by l_1, l_2, l_3 and l_4 (see Fig. 8 a). It is impossible to know which of them lies in the 1st (the nearest lamella), in the 2nd, in the 3rd or in the 4th quadrant. If one lamella is broader than the others we may assume it to be the nearest one and to lie in the 1st quadrant but we cannot be certain. Assume the lamellae l_1, l_2, l_3 and l_4 to lie in the 1st, 2nd, 3rd and 4th quadrants respectively, the angles (measured clock-wise) $l_1 \wedge l_2$, $l_1 \wedge l_3$ and $l_1 \wedge l_4$ correspond to $\alpha_{1,2}$, $\alpha_{1,3}$ and $\alpha_{1,4}$ which are computed according to the formulae deduced above. But if for instance lamella l_3 lies in the 2nd quadrant and l_2 in the 3rd quadrant the angles $l_1 \wedge l_3$, $l_1 \wedge l_2$ and $l_1 \wedge l_4$ correspond to $\alpha_{1,2}$, $\alpha_{1,3}$ and $\alpha_{1,4}$. It is easy to see that there exists a great number of angle combinations which may correspond to the angles $\alpha_{1,2}$, $\alpha_{1,3}$ and $\alpha_{1,4}$. In order to discover the right combination we must apply a very systematic procedure.

In Table VI the possible angle combinations are arranged in 24 groups. This number of groups is obtained by measuring clockwise from a chosen

Table VI. Groups of possible angle combinations.

Group	$\alpha_{1,2}$	$\alpha_{1,3}$	$\alpha_{1,4}$
1	$l_1 \wedge l_2$	$l_1 \wedge l_3$	$l_1 \wedge l_4$
2	$l_1 \quad l_2$	$l_1 \quad l_4$	$l_1 \quad l_3$
3	$l_1 \quad l_3$	$l_1 \quad l_2$	$l_1 \quad l_4$
4	$l_1 \quad l_3$	$l_1 \quad l_4$	$l_1 \quad l_2$
5	$l_1 \quad l_4$	$l_1 \quad l_2$	$l_1 \quad l_3$
6	$l_1 \quad l_4$	$l_1 \quad l_3$	$l_1 \quad l_2$
7	$l_2 \quad l_3$	$l_2 \quad l_1$	$l_2 \quad l_4$
8	$l_2 \quad l_3$	$l_2 \quad l_4$	$l_2 \quad l_1$
9	$l_2 \quad l_4$	$l_2 \quad l_1$	$l_2 \quad l_3$
10	$l_2 \quad l_4$	$l_2 \quad l_3$	$l_2 \quad l_1$
11	$l_2 \quad l_1$	$l_2 \quad l_3$	$l_2 \quad l_4$
12	$l_2 \quad l_1$	$l_2 \quad l_4$	$l_2 \quad l_3$
13	$l_3 \quad l_4$	$l_3 \quad l_1$	$l_3 \quad l_2$
14	$l_3 \quad l_4$	$l_3 \quad l_2$	$l_3 \quad l_1$
15	$l_3 \quad l_1$	$l_3 \quad l_2$	$l_3 \quad l_4$
16	$l_3 \quad l_1$	$l_3 \quad l_4$	$l_3 \quad l_2$
17	$l_3 \quad l_2$	$l_3 \quad l_1$	$l_3 \quad l_4$
18	$l_3 \quad l_2$	$l_3 \quad l_4$	$l_3 \quad l_1$
19	$l_4 \quad l_1$	$l_4 \quad l_2$	$l_4 \quad l_3$
20	$l_4 \quad l_1$	$l_4 \quad l_3$	$l_4 \quad l_2$
21	$l_4 \quad l_2$	$l_4 \quad l_1$	$l_4 \quad l_3$
22	$l_4 \quad l_2$	$l_4 \quad l_3$	$l_4 \quad l_1$
23	$l_4 \quad l_3$	$l_4 \quad l_1$	$l_4 \quad l_2$
24	$l_4 \quad l_3$	$l_4 \quad l_2$	$l_4 \quad l_1$

Table VII. Subgroups of group 1.

Sub-group	$\alpha_{1,2}$	$\alpha_{1,3}$	$\alpha_{1,4}$
1	$l_1 \wedge l_2 + 180°$	$l_1 \wedge l_3$	$l_1 \wedge l_4$
2	$l_1 \quad l_2$	$l_1 \quad l_3 + 180°$	$l_1 \quad l_4$
3	$l_1 \quad l_2 + 180°$	$l_1 \quad l_3 + 180°$	$l_1 \quad l_4$
4	$l_1 \quad l_2$	$l_1 \quad l_3$	$l_1 \quad l_4 + 180°$
5	$l_1 \quad l_2 + 180°$	$l_1 \quad l_3$	$l_1 \quad l_4 + 180°$
6	$l_1 \quad l_2$	$l_1 \quad l_3 + 180°$	$l_1 \quad l_4 + 180°$
7	$l_1 \quad l_2 + 180°$	$l_1 \quad l_3 + 180°$	$l_1 \quad l_4 + 180°$

lamella the smallest angles between this lamella and the other three lamellar systems in turn. It is not certain, however, that these angles correspond to the true values of $\alpha_{1,2}$, $\alpha_{1,3}$ and $\alpha_{1,4}$. If for instance l_1 and l_2 lies in the 1st and 2nd quadrants respectively, either of the angles $l_1 \wedge l_2$ or $l_1 \wedge l_2 + 180°$ corresponds to $\alpha_{1,2}$, which is evident from the assumptions made in deducing the formulae above. In this manner we obtain in each group 7 subgroups, whose types are demonstrated in Table VII. Thus we are concerned with in all 192 possible angle combinations, only one of which generally corresponds to the true values of $\alpha_{1,2}$, $\alpha_{1,3}$ and $\alpha_{1,4}$.

To begin with we can exclude most of the angle combinations by studying the mutual spheres of existence for the different α-values. From diagrams I and II we obtain the limiting condition I

α) *for the octahedron case,*

if	$21° < \alpha_{1,2} < 120°$,	then	$96° < \alpha_{1,3} < 180°$	and	$150° < \alpha_{1,4} < 270°$,
»	$90 < \alpha_{1,2} < 212$,	»	$180 < \alpha_{1,3} < 264$	»	$240 < \alpha_{1,4} < 337$,
»	$206 < \alpha_{1,2} < 306$,	»	$248 < \alpha_{1,3} < 360$	»	$318 < \alpha_{1,4} < 360 + 60°$,
»	$300 < \alpha_{1,2} < 360 + 41°$,	»	$0 < \alpha_{1,3} < 113$	»	$54 < \alpha_{1,4} < 153$,

β) *for the Muonionalusta case,*

if	$34° < \alpha_{1,2} < 122°$,	then	$95° < \alpha_{1,3} < 180°$	and	$148° < \alpha_{1,4} < 270°$,
»	$90 < \alpha_{1,2} < 212$,	»	$180 < \alpha_{1,3} < 266$	»	$238 < \alpha_{1,4} < 328$,
»	$206 < \alpha_{1,2} < 311$,	»	$253 < \alpha_{1,3} < 360$	»	$317 < \alpha_{1,4} < 360 + 56°$,
»	$303 < \alpha_{1,2} < 360 + 43°$,	»	$0 < \alpha_{1,3} < 107$	»	$49 < \alpha_{1,4} < 154$.

As may be seen the two schemes above are very similar and in general, the same combinations are excluded in both cases.

On writing down all possible groups from the angle determination it is easy from the schemes above to exclude whole groups together with their subgroups which contain no feasible combinations. Next we write down the remaining groups with their subgroups and exclude all combinations which are impossible according to the schemes above. In each such group we find at the most one or two possible combinations. After these exclusions there remain only about 15—30 possible combinations which must be tested in diagrams I or II.

Using diagrams I and II we have, for a given angle combination, to find a ϱ-value which gives us simultaneously for the three angles the same φ-values in the three curve-groups. If we cannot find such a ϱ-value with the angle combination the combination is impossible and the angles do not correspond to the true values $\alpha_{1,2}$, $\alpha_{1,3}$ and $\alpha_{1,4}$. In most cases we are concerned with

angle combinations which nearly coincide with the desired conditions but if the coordinates of the section lie too near to the lamella in the 1st quadrant to be probable (there is little probability that four lamellar systems are visible on sections near one lamella) the combinations must be excluded. If we exclude all sections which lie only 10°—15° from one lamella we can exclude angle combinations which give coordinates whose φ- and ϱ-values simultaneously lie within the following limits (limiting condition II)

α) *for the octahedron case,*

$$35^\circ < \varphi < 55^\circ$$
$$44^\circ < \varrho < 64^\circ,$$

and

β) *for the Muonionalusta case,*

$$35^\circ < \varphi < 55^\circ$$
$$39^\circ < \varrho < 59^\circ.$$

After the last mentioned exclusions there may remain only 1—3 possible combinations, the most probable of which is the one which gives nearly identical φ-values. In some cases, 2 or 3 angle combinations may give nearly identical φ-values (see the text below).

It is possible that for some given sections, the problem cannot be solved uniquely, but such cases must be very rare. It is not proposed to present here a detailed study of the possibilities of finding ambiguous solutions. Should such solutions be found it is better to choose another section for angle determinations.

However, it must be remarked in this connection that according to the octahedron case we obtain three solutions if a chosen section should lie in any one of the zones [100], [010] or [001]. Thus if for an angle combination we obtain a solution for the coordinates (ϱ, 0) in the zone [100] we have angle combinations also for the coordinates ((90—ϱ), 90) in the zone [010] and (90, ϱ) in the zone [001]. It is easy to prove this fact from equations (7)—(15). From a crystallographic point of view the three solutions in question are identical.

In a similar manner for the Muonionalusta case we obtain two solutions if a chosen section should lie in any one of the zones [100] and [010]. The two solutions are identical from a crystallographic point of view.

On some sections it is difficult to distinguish between the octahedron and the Muonionalusta case. As is easily understood by studying the diagrams those sections which lie nearly perpendicular to the c-axis are not convenient. Consequently it is better not to choose sections on which one pair of lamellar systems lies nearly perpendicular to the other.

d) Some examples.

α) *Section H.*

HÖGBOM assumed that the lamellar system which formed on this section a very acute (8°) angle with another, more conspicuous system was a twin, parallel to an octahedral face. This does not seem to be the case. The lamellar system in question is a fourth one which lies nearly parallel to the section and is therefore difficult to discern.

On the photograph (Fig. 3 of HÖGBOM's paper) we can measure the following angles

$$l_1 \wedge l_2 = 8.2^\circ \pm 0.8^\circ, \quad l_1 \wedge l_3 = 50.0^\circ \pm 0.6^\circ, \quad l_1 \wedge l_4 = 130.4^\circ \pm 0.5^\circ$$

or

$$l_1 = 0^\circ, \quad l_2 = 8.2^\circ, \quad l_3 = 50.0^\circ \text{ and } l_4 = 130.4^\circ.$$

On writing down the angle combinations according to Table VI, we can exclude groups 2, 3, 6, 7, 10, 12, 14, 15, 17, 19, 21 and 24. In the remaining groups we have 20 subgroups which are possible angle combinations. Of these, 18 subgroups either are quite impossible or are impossible on account of their coordinates lying too near to one lamella. Only in groups 5 (possibly) and 9 we have two remaining combinations. They are

	$\alpha_{1,2}$	$\alpha_{1,3}$	$\alpha_{1,4}$	
1)	310.4°	8.2°	50.0°	Group 5, subgroup 1
2)	302.2	351.8	41.8	» 9, » 1.

In diagram II the first angle combination gives small differences when $\varrho = 60^\circ$; $\varphi = 44.2^\circ$ for $\alpha_{1,2}$; $\varphi = 43.1^\circ$ for $\alpha_{1,3}$; $\varphi = 45.8^\circ$ for $\alpha_{1,4}$. For larger values of ϱ the differences between the three φ-values increase, for smaller values of ϱ the differences decrease but in these cases we obtain a less probable combination because it falls inside the limits defined above (limiting condition II).

The second angle combination gives, when $\varrho = 65.5^\circ$ the smallest differences between the φ-values. They are $\varphi = 47.5^\circ$ for $\alpha_{1,2}$; $\varphi = 48.0^\circ$ for $\alpha_{1,3}$; $\varphi = 48.5^\circ$ for $\alpha_{1,4}$. Thus the second combination must be considered as the most probable one and we have the coordinates for the section

$$\varphi = 48^\circ$$
$$\varrho = 65^\circ.$$

The section was supposed by HÖGBOM to lie parallel to (110). In reality it lies between (110) and (111), but nearer to (111).

In group 9 (see Table VI) lamella l_1 lies in the 3rd, l_2 in the 1st, l_3 in

the 4th and l_4 in the 2nd quadrant. Consequently l_2 is the lamellar system which is nearest the section and for this reason it appears less distinct than the others.

β) *The c_1-face of sample 1.*

The c_1-face of sample 1 is a face with four lamellar systems visible. According to Table II we have

$$l_1 = 232.8^\circ, \quad l_2 = 235.0^\circ, \quad l_3 = 103.1^\circ, \quad l_4 = 183.6^\circ$$

or

$$l_1 = 0^\circ, \quad l_2 = 2.2^\circ, \quad l_3 = 230.3^\circ, \quad l_4 = 310.8^\circ.$$

Groups 2, 3, 6, 7, 10, 12, 13, 14, 15, 17, 19, 21, 23 and 24 are excluded. In the remaining groups 18 subgroups are then possible. Of these, 16 subgroups are excluded according to the limiting condition II. The remaining subgroups are

	$\alpha_{1,2}$	$\alpha_{1,3}$	$\alpha_{1,4}$				
1)	310.8°	2.2°	50.3°	Group	5,	subgroup	4
2)	308.6	357.8	48.1	»	9,	»	4.

The first angle combination gives, when $\varrho = 76.1^\circ$ the smallest differences between the φ-values. For $\alpha_{1,2}$ $\varphi = 44.6^\circ$; for $\alpha_{1,3}$ $\varphi = 44.2^\circ$; for $\alpha_{1,4}$ $\varphi = 44.8^\circ$. The second combination gives, when $\varrho = 75.0^\circ$; for $\alpha_{1,2}$ $\varphi = 45.9^\circ$; for $\alpha_{1,3}$ $\varphi = 45.8^\circ$; for $\alpha_{1,4}$ $\varphi = 45.9^\circ$. Although it is difficult to judge, the second combination seems to be the most probable one and thus the coordinates are

$$\varphi = 46^\circ$$
$$\varrho = 75^\circ$$

which agrees very well with the values previously found ($\varphi = 46^\circ$, $\varrho = 74^\circ$. See Fig. 6).

As in the preceding example the most probable angle combination belongs to group 9. Lamella l_1, corresponding to lamella II (see Table II) lies consequently in the 3rd quadrant; l_2, corresponding to I in the 1st; l_3, corresponding to III in the 4th; and l_4, corresponding to IV in the 2nd quadrant. All in good accordance with the determinations in Chapter I (see Fig. 6).

γ) *The e_2-face of sample 2.*

The e_2-face of sample 2 is also a face having four lamellar systems visible. According to Table IV we have

$$l_1 = 181.0^\circ, \quad l_2 = 185.9^\circ, \quad l_3 = 249.7^\circ, \quad l_4 = 267.4^\circ$$

or

$$l_1 = 0^\circ, \quad l_2 = 4.9^\circ, \quad l_3 = 68.7^\circ, \quad l_4 = 86.4^\circ.$$

Groups 3, 5, 6, 10, 13, 14, 20 and 22 are excluded. Groups 1, 2, 11, 12, 15, 17, 19, 21 as well as 14 subgroups are then possible. Of these, 6 groups and 14 subgroups are impossible or are excluded according to limiting condition II. The remaining groups are

	$\alpha_{1,2}$	$\alpha_{1,3}$	$\alpha_{1,4}$	
1)	4.9°	68.7°	86.4°	Group 1
2)	355.1	63.8	81.5	» 11.

The first angle combination gives, when $\varrho = 79.0^\circ$ the smallest differences between the φ-values. For $\alpha_{1,2}$ $\varphi = 3.9^\circ$; for $\alpha_{1,3}$ $\varphi = 9.8^\circ$; for $\alpha_{1,4}$ $\varphi = 6.7^\circ$. The second combination gives, when $\varrho = 84.5^\circ$; for $\alpha_{1,2}$ $\varphi = 8.9^\circ$; for $\alpha_{1,3}$ $\varphi = 12.4^\circ$; for $\alpha_{1,4}$ $\varphi = 10.8^\circ$. The second combination seems to be the most probable one and thus the coordinates are

$$\varphi = 11^\circ$$
$$\varrho = 84^\circ$$

which agrees well with the values previouslv found ($\varphi = 12^\circ$, $\varrho = 84^\circ$. See Fig. 6).

The most probable angle combination belongs to group 11. Lamella l_1, corresponding to lamella II (see Table IV) lies consequently in the 2nd quadrant; l_2, corresponding to IV in the 1st; l_3, corresponding to III in the 3rd; and l_4, corresponding to I in the 4th quadrant. All in good accordance with the determinations in Chapter I (see Fig. 6).

e) Remarks on the method.

The examples chosen above can be brought in accordance only with diagram II for the Muonionalusta case. The deviations are mostly very pronounced if the values are tried in diagram I. The author has had little opportunity to expand the investigation and test the diagrams on samples from other octahedrites but hopes that the diagrams may be of value to those who are interested in the subject. At any rate it seems to be important to ascertain in a simple manner whether a given material under investigation is a true octahedrite or not.

In an appendix at the end of this article the method has also been used for determining the orientation and type of some other meteoric irons.

CHAPTER III.

Microstructure of the Muonionalusta iron meteorite.

a) Structure elements.

As suggested by HÖGBOM the Muonionalusta meteorite belongs to the group of fine octahedrites ("Oktaedrite mit feinen Lamellen"). According to F. BERWERTH's system of classification (5) the meteorite is placed in the group of octahedrites with three constituents, namely kamacite-plessite-taenite and in view of the lamellar width, in the subgroup "fine octahedrites rich in plessite". If for the present we ignore the fact that the meteorite does not represent a true octahedrite we must accept the above-mentioned classification although the meteorite in some respects closely resembles the medium octahedrites the width of whose kamacite lamellae > 0.5 mm. The mean value of the width of the kamacite lamellae seems to be about 0.4—0.5 mm, but mostly on the small side. The Ni-content (8.02 %) however, is smaller than that of most of the fine octahedrites (> 9 % Ni). In this respect as well, the meteorite seems to be a transitional form between a fine and a medium octahedrite.

The width of the kamacite lamellae ranges from 0.2 to 0.7 mm. The broadest lamellae are mostly those which lie together in a parallel arrangement and which are separated from one another only by narrow ribbons of taenite. By virtue of this fact those kamacite lamellae which are bordered on either side by the other two constituents are the narrowest ones (see the Plate, Fig. 1)[1], while such as are bordered on only one side by taenite and plessite are generally somewhat broader (see Fig. 2).

The narrow ribbons (width mostly 0.01—0.02 mm) of taenite are mostly very sharply defined (see Fig. 2), but they often seem to be diffuse. Sometimes they appear corroded especially along the boundaries between the kamacite and plessite. In such cases they tend at some points along the boundary between the kamacite and plessite to have swollen into a triangular shape with the sharp vertex directed towards the plessite (see Fig. 3 and Fig. 1). The structure is described by F. RINNE and H. E. BOEKE (6) and is called "cone structure" (Zapfenstruktur). This structure is but rarely observed within a kamacite lamella.

The interstices between the kamacite plates are filled mostly with plessite which shows numerous forms of development. Sometimes however, relatively small aggregates of plessite are wholly enclosed by only one kamacite lamella. The area of the angular interstices with plessite has in general a magnitude of 1—5 sq mm. There are two main forms of plessite, one of which is fine with no structure visible at low magnifications while the other is much coarser

[1] The Figures in this chapter refer to the Plate XIX.

with narrow kamacite plates (width 0.01—0.10 mm) separated by very narrow ribbons of taenite (width < 0.01 mm, see Fig. 4). According to E. PFANN (7) the first form is supposed to correspond to true eutectoid plessite while the other form to a macroplessite or microoctahedrite. The macroplessite does not always have the more or less distinct octahedral structure as in Figure 4 but may consist of narrow kamacite plates in a parallel arrangement as is shown in Figure 5. At greater magnifications the fine eutectoid plessite shows a peculiar reticular structure (see Fig. 6). The fine eutectoid plessite is the most frequent. Only occasionally does a whole plessite aggregate consist solely of macroplessite. It is common, as in Figure 4 and 6, for both forms to appear together in a plessite aggregate and various transitional forms may be seen at the boundaries between the two main forms.

b) Constitution and microstructure.

With the aid of a Leitz' integral micrometer disc volumetric estimations of the three constituents kamacite, taenite and plessite was executed on four of the faces of the Muonionalusta iron meteorite. The results of these estimations are shown in Table VIII below.

Table VIII. Volume-percentages of the three constituents of the Muonionalusta iron meteorite.

Face	Kamacite	Taenite	Plessite
c_1	80.5 %	4.6 %	14.8 %
c_2	78.5	4.2	17.3
d_1	82.2	3.6	14.2
e_2	81.8	3.5	14.7
Mean values	80.8	4.0	15.2

In order to form some idea of nickel content of the three constituents from the volumetric analyses we must know the densities of the constituents and the composition and density of the meteorite. The chemical composition as well as the density has been determined by R. MAUZELIUS (see HÖGBOM's paper) who obtained the following result:—

Fe	91.10 %
Ni	8.02
Co	0.69
Cu	0.01
Cr	0.01
P	0.05
	99.88

Density (at 21° C) = 7.893 gr cm^{-3}

The most accurate value of the density of kamacite seems to be that calculated from the X-ray determinations by E. R. JETTE and R. FOOTE (8) who for the α-phase (kamacite) of samples of iron-nickel containing 5.16 atomic per cent (5.41 wt per cent) Ni found the lattice constant to be $a_0 = 2.8634$ Å. From this we calculate the density = 7.870 gr cm^{-3}. The same authors have also examined the γ-phase (taenite) of specimens containing 24.81 (25.75), 28.59 (29.62), 33.80 (34.92) and 39.16 atomic per cent (40.31 weight per cent), and found the lattice constants to be $a_0 = 3.5727$, 3.5755, 3.5862 and 3.5884 Å respectively. From these values the densities 8.185, 8.182, 8.129 and 8.144 gr cm^{-3} are calculated. Even in the mentioned Ni-content range a pronounced anomaly appears in the density curve of JETTE and FOOTE. Taking the mean value we obtain a density = 8.160 gr cm^{-3} for taenite. For plessite we have no determinations but if we choose for this constituent the mean value of the densities of kamacite and taenite or 8.015 gr cm^{-3}, the density of the Muonionalusta meteorite with the above determined volumetric composition is calculated to be

$$7.903 \text{ gr cm}^{-3}.$$

As may be seen the figure of the calculated value is somewhat larger than that determined by MAUZELIUS. Besides the obvious uncertainty in choosing the densities of the constituents, the small discrepancy may be due to the effect of impurities and also to an effect discovered by W. FRAENKEL and G. TAMMANN (9) in Damara iron. By heating the iron meteorite to such a high temperature (1 300° C) that the meteoric structure disappeared they found that after cooling, the density had increased (7.908—7.938 gr cm^{-3}). Meteoric irons seem in other words to have a slightly lower density than technical iron-nickel alloys of corresponding compositions.

The difference between the experimental and calculated density is at any rate so small that we may assume the errors in the above values of the densities of the constituents to be not very great. If by means of the density values, we wish to calculate the nickel contents of the three constituents from the nickel content of the Muonionalusta meteorite we may do so according to the following expression:

$$V_k d_k Ni_k + V_t d_t Ni_t + V_p d_p Ni_p = 100 d_m Ni_m, \tag{25}$$

where

V_k, V_t, V_p = volume-percentage of kamacite, taenite and plessite,

d_k, d_t, d_p, d_m = density of kamacite, taenite, plessite and of the meteorite as a whole,

Ni_k, Ni_t, Ni_p, Ni_m = Ni-content of kamacite, taenite, plessite and of the meteorite as a whole.

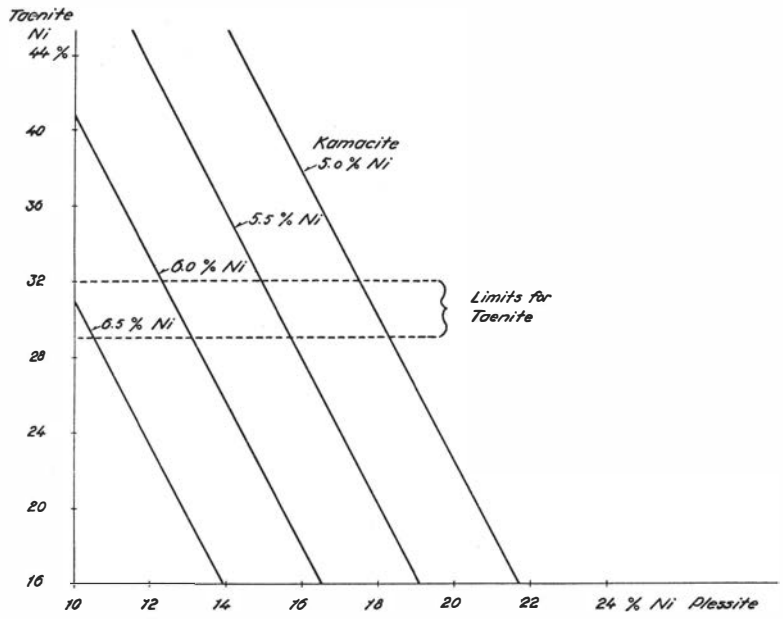

Fig. 9. Alternative compositions of the constituents kamacite, plessite and taenite of the Muonionalusta iron meteorite.

As illustrated in diagram Fig. 9[1], the Ni-contents of taenite and plessite according to equation (25) should vary linearly with a given value of the Ni-content of kamacite if we assume the Ni-content of the meteorite to be 8.02 %. In the diagram, lines of constant Ni-content are drawn for Ni-contents = 5.0, 5.5, 6.0 and 6.5 % in the kamacite. Of course the supposition that d_k, d_t and d_p are constants is not quite correct and therefore, the diagram only represents the actual conditions schematically. From the determinations of the lattice constant of kamacite in several iron meteorites, E. A. OWEN and B. D. BURNS (10) obtained a mean value corresponding to 6.2 % Ni. The same authors [see also C. BENEDICKS (11)] found for taenite lattice constants corresponding to 29—32 % Ni. As may be seen in Fig. 9 these values would give an extremely low Ni-content (12 % Ni) for plessite compared with the Ni-content (17—18 % Ni) of plessite determined by PFANN (7). If the Ni-content is as high as that proposed by PFANN the Ni-content of kamacite must be assumed to be 5.0—5.5 % or of about the same magnitude as that found in technical iron-nickel alloys.

[1] In the text.

CHAPTER IV.

Crystal chemistry of iron-nickel alloys and its application to the Muonionalusta type.

a) Some general problems.

One of the most characteristic features of octahedrites is that they mostly have very well-developed structures. The type of internal structure which on etched sections gives rise to the well-known WIEDMANNSTÄTTEN figures is a function of the chemistry of the meteorites. The existence of an octahedrite involves a Ni-content $> 5—7$ % and the width of the lamellae decreases with successively higher Ni-contents. We can formulate many rules concerning the relationship between the chemical constitution and crystal structure of octahedrites but we cannot reproduce them in the laboratory. C. BENEDICKS (12) did indeed succeed by very slow cooling of an iron-nickel alloy containing 12 % Ni in obtaining a structure slightly resembling an octahedrite.[1] In spite of this fact the following statement by R. VOGEL in "Handbuch der Mineralchemie" (page 573) still seems to be valid: "Die Erzeugung der WIEDMANNSTÄTTENschen Figuren muss aber so lange zweifelhaft bleiben, als es nicht gelungen ist, die künstlichen WIEDMANNSTÄTTENschen Figuren in vollständiger Übereinstimmung mit den meteorischen hervorzubringen und ihre Identität mit diesen letzteren durch ihre Umwandlung in die Struktur des technischen Nickeleisens beim Erhitzen nachzuweisen."[2]

Althought it is impossible to reproduce the octahedral structure artificially there is no reason to believe that the reactions necessary to form the structure can take place only in a cosmic milieu in some way. The influence of pressure for the formation of octahedrites is little known. FRAENKEL and TAMMANN (9) (who regarded meteorie irons as stable only at higher temperatures) was of the opinion that, if the formation of the octahedral structure had taken place at a high pressure, the density of meteorie irons must be higher than that of technical iron-nickel alloys of corresponding compositions. In reality it is lower (see pag. 303) and thus the formation has not occured at a high pressure. The temperature at which the structures are formed appears, as already pointed out by BENEDICKS (11), to be rather low instead of high and lies probably much below the solidus and liquidus curves of the Fe—Ni equilibrium diagram. There remains the

[1] A synthesis closer resembling an octahedrite has more recently been made by R. F. MEHL and G. DERGE (see F. A. PANETH, The Origin of Meteorites. Halley Lecture. The Clarendon Press, Oxford 1940, Plate III, p. 17).

[2] Transl.

"The ability to produce W. structures must however be regarded as doubtful until it has been possible to effect either complete accordance between synthetic and meteoric W. structures or to prove their identity with the latter by studying their transformation, on heating, in the structure of technical nickel iron alloys."

rate of cooling, as one of the factors of octahedrite formation, to be taken into consideration. The most outstanding reason why our present knowledge of the equilibrium conditions for iron-nickel is still not satisfactory seems to be the sluggishness of the atomic diffusion in the Fe-Ni system especially at lower temperatures. This fact is emphasized by almost all investigators who have in more recent times worked with alloys belonging to this system.

All the problems concerning the mode of formation of octahedrites can hardly be discussed in detail in this article. The discussion must be restricted to treat the general question whether the newly discovered structural arrangement of the Muonionalusta iron can contribute to a better understanding of its formation or if it makes the subject even more complicated. To begin with it seems advantageous to offer a brief review of the theories up to the present time.

b) Theories concerning the formation of octahedrites and their relation to different phase diagrams of iron-nickel.

In order to explain the structures of iron meteorites F. OSMOND and G. CARTAUD (13) supposed that γ-iron and β-nickel were completely miscible in both the liquid and solid state. α-Fe and α-Ni however, were not miscible in all proportions. According to their phase diagram made in collaboration with F. ROOZEBOOM there exists a miscibility gap in the solid state between 6—33 % Ni where the iron-nickel alloy is split up into two phases whose compositions correspond to those of kamacite and taenite. As the iron-nickel alloy cools one of the phases separates out so that at about 350° C a eutectic point is reached at which a duplex mixture separates having the composition of plessite. Furthermore they supposed that the diagram could be applied to meteorites as well as to technical iron-nickel alloys; in the latter case however, the duplex structure would be sub-microscopic and therefore not distinguishable.

According to OSMOND's hypothesis it was among other things difficult to explain why taenite was formed from compositions on the Fe-side of the eutectic point or why primary taenite was not formed on the Ni-side of the same point. The hypothesis was critizised by FRAENKEL and TAMMANN (9) but supported in principle by D. HANSON and H. E. HANSON (14) and by D. HANSON and J. R. FREEMAN (15). In the light of more modern structure researches, above all those of JETTE and FOOTE (8), A. J. BRADLEY and H. J. GOLDSCHMIDT (16), E. A. OWEN and A. H. SULLY (17) the validity of the hypothesis can no longer be confirmed, at any rate not in certain important respects. The suggestion by OSMOND that the Fe-Ni-system is a two phase system is nowadays accepted as being correct while the supposition of a one-phase system by FRAENKEL and TAMMANN is held to be wrong. However, X-ray analyses do not indicate the existence of a eutectoid.

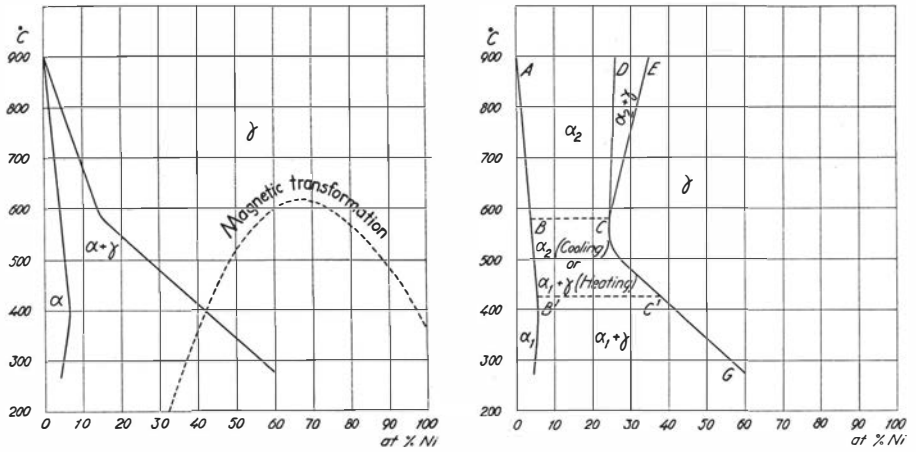

a b

Fig. 10. Equilibrium diagrams of iron-nickel according to OWEN and SULLY.

According to the phase diagram of OWEN and SULLY (see Fig. 10 a) iron-nickel alloys of compositions from 6 % Ni is split up into two phases over a very wide two-phase region. The Ni-poor α-phase (corresponding to kamacite in iron meteorites) represents a body-centred cubic lattice and the Ni-rich γ-phase (corresponding to taenite) a face-centred cubic lattice. The phase diagram shown in Fig. 10 a was obtained by studying the equilibrium conditions at high temperatures with the aid of a special high temperature camera. By quenching or slowly cooling the specimens OWEN and SULLY found the conditions more complicated and the results from these investigations is illustrated by them within the diagram, Fig. 10 b. In a few words the results may be summarized as follows. Specimens of Fe-Ni alloys with a Ni-content less than 6 % consist when quenched from a moderately high temperature, of an ordinary body-centred α-phase structure, designated by α_1. If however, the specimens contain more nickel, viz. between 8—23 % Ni they consist, if annealed at say 900° C for some days, slowly cooled to 500° C and then quenched, of an α_2-structure which may be described as a distorted body-centred α-phase structure. If the same specimens are heated to say 500° C, held at that temperature and then quenched a mixture of the α_1- and γ-phase is obtained. Finally, specimens with a higher Ni-content ($>$ 27 % Ni) consist as a rule when quenched from high temperatures only of the γ-phase or, when quenched from lower temperatures, of mixtures of the α_1- and γ-phase. Concerning the α_2-structure OWEN and SULLY make in this connection the very curious remark (page 618): "The distorted α_2-structure corresponds to the material which Hanson calls 'martensite' owing to its resemblance to martensite in carbon steel, although the structures are not similar — the latter being tetragonal, whilst the former is cubic." We shall return to this passage in the discussion later on.

BRADLEY and GOLDSCHMIDT who investigated the equilibrium conditions of quenched specimens of iron-nickel alloys, obtained results similar to OWEN and SULLY. They also showed the existence of two body-centred cubic structures α and α_1 of which α_1 seems to correspond to the α_2-structure of OWEN and SULLY. They assumed the α_1-structure to be a new phase and discussed whether this phase could possibly correspond to an ordered atomic arrangement or a superlattice with a composition near Fe_3 Ni. Finally they raise the question if there also exist a second γ-structure or γ_1.

The present review of theories would be incomplete without mentioning the recently published article on the subject by BENEDICKS (11). According to him we have to seek the mode of formation of octahedrites in the fact that the solubility of Ni in the α-phase increases with decreasing temperature at temperatures above 380° C. At lower temperatures however, the solubility decreases with decreasing temperature and at 380° C where the solubility is at a maximum, there is a sharp break in the phase boundary line between the α- and $(\alpha + \gamma)$ -fields of the equilibrium diagram (see Fig. 10 a). If now a meteoric iron with a Ni-content > 6 % is cooled very slowly we have reason to expect the separation of a relatively Ni- poor α-phase from a Ni- rich γ-phase. The α-phase is separated as kamacite lamellae parallel to the octahedral planes. As the temperature of the meteorite decreases the Ni- content of the kamacite lamellae increases in the outer layers until a temperature of 380° C is reached. If the temperature decreases still further a γ-phase is separated inside the Ni-rich outer layers of the kamacite forming taenite lamellae while the parent γ-phase which fills up the interstices between the kamacite lamellae, is split up into an α- and γ-phase depending on the degree of supersaturation of the α-phase. According to this hypothesis plessite is formed thus.

Concerning the formation of taenite the hypothesis proposed by BENEDICKS is similar to the older hypothesis of RINNE (18) who suggested that the separation of taenite was due to a change in solubility ("Rückschlagsbildung") at a temperature below the eutectoid point. However this hypothesis has been brought into better accordance with modern viewpoints on the equilibrium conditions of the iron-nickel system.

c) Does the Muonionalusta structure represent traces of a tetragonal phase?

Without an exact knowledge of the reason it has been assumed *a priori* that in some manner the lamellar orientation of octahedrites is controlled by the γ-phase whose planes of closest atomic packing are parallel to the octahedral planes. But if now in one case at least it is shown that the lamellar orientation does not correspond to the octahedral structure the question may arise whether the lamellar orientation in such cases has been influenced by another modification of the iron-nickel system or whether the tetragonal

structure is an arrangement formed by a mere change. This last possibility seems to be the less probable one. If accepted, the formation of octahedrites should be even more mysterious than ever. The fact that the structure is built up in an arrangement governed by crystallographic laws also speaks against this possibility.

The assumption that there exists, or has existed during the cooling process, a tetragonal phase of meteoric iron seems to be rather bold because no evidence of the existence of such a phase is given by X-ray analysis of either technical iron-nickel alloys or meteoric irons. Not many X-ray investigations of meteoric irons have been performed but a few are available. The most extensive X-ray studies were carried out by OWEN and BURNS (10) who for the purpose have used specimens from the museum of Harvard University and from the British Museum. Among the 24 specimens 8 octahedrites are represented.

From the material investigated OWEN and BURNS found only the α- and γ-phase and among the ataxites a few cases where the above-mentioned distorted α_2-structure was present. They do actually mention diffuse or faint lines in the spectra obtained but these are interpreted as being caused by small impurities or by the material having been »cold worked» during sampling. The diffuse α-lines seem to disappear if the specimen is carefully annealed at 350° C. The γ-lines however, may remain diffuse even after such a treatment.

At any rate the results of OWEN and BURNS indicate that there is but little chance of establishing the existence of the assumed tetragonal phase with X-ray analysis of meteoric iron at room temperature. Because of this we have reason to conclude that the tetragonal modification is a metastable form which is transformed completely at room temperature. In this respect the tetragonal form seems to be less stable than the α_2-structure which is not stable at low temperatures as shown by OWEN and BURNS. An annealing treatment at so low a temperature as 250°—300° C is sufficient to break up the α_2-structure of meteoric iron into its α- and γ-components. It is possible that the tetragonal modification has something to do with the α_2-structure and that it may be a transitional form between the γ-structure and the α_2-structure. Probably there is a very restricted temperature range in which it is stable. In spite of the general sluggishness which is characteristic for iron-nickel alloys the stability of the tetragonal modification may be so slight that it transforms relatively rapidly. Therefore the modification cannot be established on quenched material. Or it may also be possible that the rate of formation of the modification is so slight that only an exceedingly small quantity is formed by such rapid cooling. The only chance of reproducing the modification may be to cool the specimens very slowly, possibly so slowly that it is impracticable to carry it out in the laboratory. During the cooling process X-ray analysis must simultaneously be carried out with a high temperature camera.

d) The lattice of the assumed tetragonal modification.

If we have some reason for assuming the existence of a tetragonal phase during the cooling process of the Muonionalusta iron we may discuss how the lattice of this phase has been built up. Thus we may discuss the following possibilities.

The tetragonal phase is α) a superstructure,
β) an interstitial structure,
γ) simply a tetragonal space-lattice of the BRAVAIS type.

α) *The possibility of a superstructure.*

Metals, especially true metals, have generally very simple crystal structures of high symmetry. Besides, in alloy systems of two or more true metals the lattices mostly have a cubic or hexagonal symmetry often in close-packed atomic arrangements. In substitutional alloys of say two components forming solid solutions of one component in the other, the lattices are also built up in a highly symmetrical manner whereby atoms of the one component quite randomly are replaced by atoms of the other. The substitution of atoms can in this manner occur over a very wide range of chemical composition of the alloys without the structures of the space-lattices being transformed. Within such ranges only the parameters of the unit cells vary with composition. Within ranges of a mostly much narrower width however, the atomic distribution may proceed from a disordered to an ordered arrangement which is followed by a discontinuous transformation of the structure of the space lattice. In this way a so-called superlattice is formed. The tendency to form a superlattice is strongly pronounced when the alloys have chemical compositions in which the atomic contents of the components can be expressed as fractional numbers which are small integers.

The rule has been proposed that the probability of obtaining superlattices in alloy systems is small if the atomic radii of the components are equal. A large difference in the size of the atoms, too, decreases this probability. Therefore the probability for superlattices to be formed is greatest if the sizes of atoms of the components are not equal but differ to some extent.

Compared to the simple lattice structure of the components the superlattice is more complicated. It has a greater unit cell with a relatively greater number of atoms. It may generally be considered as being built up of two or more interpenetrating space-lattices, each containing one kind of atom only. If the atomic radii of the components are different the superlattice often has a lower symmetry than the lattices of the components. This seems to be dependent on the fact that in the metallic state the atoms are very closely packed together and if the sizes of atoms are different the lattice of a

lower symmetry really does represent an arrangement of closer packing than is possible in an arrangement of higher symmetry as for instance in the tetragonal superlattice of copper and gold studied by C. H. JOHANSSON and J. O. LINDE (19).

Taking into consideration the above mentioned factors concerning the formation of superlattices we maintain that the probability of superlattices being formed in the Fe-Ni alloy system is small. The sizes of the Fe- and Ni-atoms are almost equal. The difference between the atomic radii of the components does not seem to exceed 2 to 3 % of the total radii. Nevertheless P. LEECH and C. SYKES (20) report that they have found indications of the existence of a superlattice of a composition near Ni_3Fe. The evidence however, appears to be a little uncertain. As mentioned earlier BRADLEY and GOLDSCHMIDT (16) have discussed the possible existence of a superlattice near Fe_3Ni and BENEDICKS (11) and other authors the possibility of a superlattice in the region of Fe_2Ni. The last mentioned superlattices have never been observed unless they correspond to the observed distorted structures.

In this connection it may be added that the above-mentioned empirical rule may possibly be wrong to some extent. Even in the case of atoms of equal size it is, or at any rate, it has been very difficult with the aid of X-ray analysis to establish the existence of a superlattice built up of two or more different atoms of equal size and because of this the rule has been formulated for the case of such alloy systems. In other words, in these alloy systems we really may have superlattices but they have not been established. In the Fe-Ni system we are concerned with atoms of both equal size and similar scattering power for X-rays of different wave-lengths.

However, the above-mentioned viewpoints cannot change our conception that it is unprobable that the tetragonal phase is a superlattice. If then superlattices really do exist in the Fe-Ni system there is little chance that they would have a lower symmetry because of the equal sizes of the Fe- and Ni-atoms. At the most we may expect a little distortion in the cubic symmetry in such superlattices.

β) *The possibility of an interstitial structure.*

The structural properties of iron meteorites have often been compared with those of carbon steel. As already pointed out the α_2-structure (see p. 307) was compared with martensite and in the same manner the γ—α transformation of nickel-iron alloys has been considered to be more or less identical with the austenite-ferrite transformation of carbon steel. The comparison is mainly based on some similarities obtained in microscopic studies on polished sections of samples but we shall not here discuss how justified such a general comparison may be. In the case of the Muonionalusta iron the subject is of interest because it lies near at hand to assume that the tetragonal phase is of the same lattice type as tetragonal martensite.

According to modern viewpoints martensite is considered as being an interstitial α-iron lattice where the small carbon atoms are placed in the interstices between the larger iron atoms. The martensite structure however, does not represent a normal interstitial lattice because the carbon atoms have not sufficient space in the interstices between the iron atoms. Nevertheless, the iron has taken up some carbon but whether the carbon atoms are distributed at random or according to some special scheme does not seem to be quite clear. The martensite lattice is supersaturated with carbon atoms and the large content of carbon is considered to have caused the distortion of the cubic lattice. The larger the carbon content is the more the lattice is distorted while in the case of small carbon contents the lattice is cubic and no martensite is formed.

The fact that the Muonionalusta iron evidently contains very little carbon speaks against the possibility of explaining the tetragonal phase as an interstitial structure of the martensite type. We have, too, no reason to expect the tetragonal phase to be an interstitial structure of a normal type or of the so called X_2-structure type. In the first mentioned structure type the lattices have often but not always the same lattice structure as the lattice of the pure metal without interstitial non-metallic atoms. The symmetry is mostly cubic or hexagonal as has been shown by G. HÄGG in a couple of investigations concerning this subject.

γ) *The possibility of a tetragonal space-lattice of the* BRAVAIS *type.*

Having stated that there is little possibility of explaining the tetragonal phase as a superlattice or an interstitial lattice we are left with the choice of examining if it corresponds to a simple space-lattice of the BRAVAIS type. The motive for such an assumption requires a further explanation. As is known the total symmetry of crystalline matter is dependent on two facts, viz. on the symmetry of the basement space-lattice and on the symmetry of the mass points or particles which form the constituents of the lattice. Usually it is imagined that the constituting mass points are situated in space like the knots of a net-work, the meshes of which are the congruently arranged parallelopiped cells. In homodesmic crystals with metallic bonds the corners and occasionally some other specific positions of the parallelopiped cells — mostly built up in a simple manner — are occupied by single atoms which approximately may be considered as mathematical points. In such monatomic metallic crystals the systems of BRAVAIS are almost without exception sufficient to describe the symmetry qualities of the lattice. In the case of crystals containing two or more different atoms however, it is sometimes necessary to introduce symmetry elements of the first order and accordingly, the symmetry qualities of such a lattice must be specified in the systems deduced by SOHNCKE. The SOHNCKIAN systems may be considered as being built up of congruent and parallel interpenetrating space-lattices of the BRAVAIS type.

Formally, the lattices of true metals and their alloys only represent atomic arrangements belonging to the SOHNCKIAN systems and it is unnecessary in the treatment of our special problem to introduce the space-group systems which include all possible lattice arrangements of crystalline matter. The reason why we can simplify our problem further on and only take into consideration possible lattices of BRAVAIS which naturally like the SOHNCKIAN lattices are simply special cases of space-groups, is the fact that the Ni- and Fe-atoms are of about the same size. Although it is an alloy we can consider the lattice as monatomic.

Accepting the above-mentioned viewpoints we have to choose between a simple or a body-centred tetragonal lattice. That the tetragonal phase should be built up of simple cells seems to be very improbable because the packing of the atoms cannot be sufficient. The closest attainable packing in a primitive cell with the determined axial ratio is about 0.42. This means that the material must expand about 75 per cent during the transformation to the tetragonal phase, which is inconceivable.

In the closest primitive cells of tetragonal symmetry a 4-fold co-ordination should exist. This co-ordination is too low and we must expect at least an 8-fold co-ordination. It is possible to attain such a high co-ordination in a body-centred tetragonal cell. The mathematical expression for the condition of an 8-fold or higher co-ordination is

$$kr\sqrt{2+\left(\frac{c}{a}\right)^2}=4r \tag{25}$$

where k is the length of the unit cell along the a- and b-axes, measured in atomic radius r as unit. Hence $\frac{c}{a}\cdot k$ is the length of the unit cell along the c-axis (see Fig. 11).

The conditions for the existence of such a body-centred tetragonal cell is further

$$\left.\begin{aligned} k &\geqq 2 \\ \frac{c}{a}\cdot k &\geqq 2 \end{aligned}\right\} \tag{26}$$

and

From inequalities (26) and equation (25) the limits within which the cell exists can be calculated. They are

$$\sqrt{\frac{2}{3}} \leqq \frac{c}{a} \leqq \sqrt{2}. \tag{27}$$

If we try to deduce the packing P of the cell we obtain

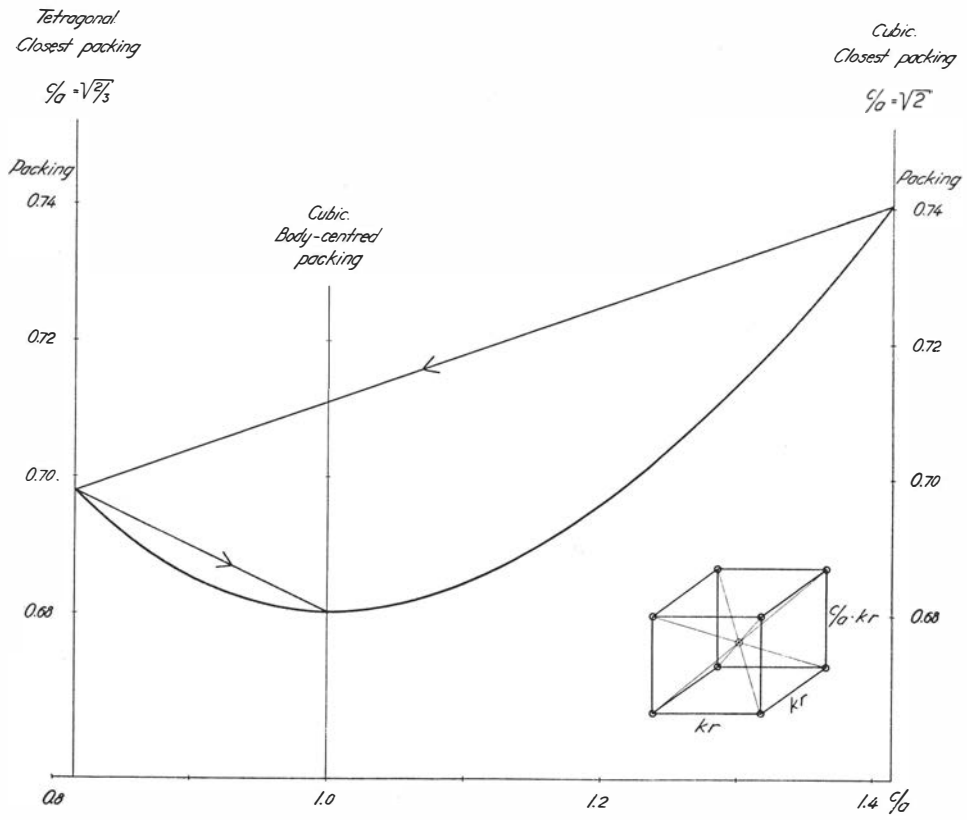

Fig. 11. Packing of atoms in a 8-fold or higher co-ordination for different $\frac{c}{a}$ values.

$$P = \frac{2\frac{4}{3}\pi r^3}{\frac{c}{a}(kr)^3}$$

or

$$P = \frac{\pi}{24} \cdot \frac{\left[2 + \left(\frac{c}{a}\right)^2\right]^{3/2}}{\frac{c}{a}} \cdot \tag{28}$$

The curve of Fig. 11, calculated according to equation (28) illustrates the closest packing of a tetragonal cell for a given axial ratio $\frac{c}{a}$ within the limits in which a tetragonal cell with 8-fold or higher co-ordination can exist. The curve is of very great interest. It shows two maxima and one minimum. The maximum point to the right at a $\frac{c}{a}$-value $= \sqrt{2}$ corresponds to the special case

where the atomic arrangement is only apparently tetragonal. In reality the arrangement is the cubic face-centred lattice with the closest cubic packing. The minimum point at a $\frac{c}{a}$-value = 1 corresponds to the special case where the cell is cubic body-centred. The maximum point to the left at a $\frac{c}{a}$-value = $\sqrt{\frac{2}{3}}$, however, represents a cell of pure tetragonal symmetry which may be called *the closest tetragonal packing*. As is illustrated in Fig. 11, it is possible to find tetragonal cells with closer packing but these cells are built up in a similar manner to the closest cubic packing and do not deviate much from it. We may call them *pseudocubic*.

It is evident *that the axial ratio of the Muonionalusta structure is the same or nearly the same as the axial ratio of the cell of the closest tetragonal packing defined above*. It is therefore reasonable to assume that the tetragonal phase has the atomic arrangement of the closest tetragonal packing.

Table IX. Comparision between the cubic metallic cells and the tetragonal cell of closest packing.

Cell	Edge lengths of the cell	Packing	Co-ordination
Cubic face-centred. Closest packing	$2\sqrt{2}\,r$ (2.84 r)	0.741	12
Tetragonal body-centred. Closest packing	$\begin{cases} c = 2r \\ a = \sqrt{6}\,r \text{ (2.45 } r) \end{cases}$	0.699	10
Cubic body-centred	$\frac{4}{\sqrt{3}}r$ (2.31 r)	0.680	8

In Table IX the cubic face-centred and the cubic body-centred cells which are the commonest ones in the metallic state are compared with the tetragonal cell of closest packing. As is obvious from the Table the tetragonal cell is in all respects an intermediate form between the two cubic cells. This fact is a point justifying the suspicion that the tetragonal phase is a transitional form between the γ- and α-phase.

The behaviour of the lattice during the transformation from the γ- to the α-phase of iron is studied above all in connection with the martensite-formation of carbon steel. The more complex scheme for that transformation does not, according to G. V. SMITH, R. F. MEHL (21) and other authors appear to be valid for an iron-nickel alloy of the Muonionalusta type. Neither does the simpler scheme proposed by P. NIGGLI (22) for the γ—α-transformation of iron seem to be applicable. In the Muonionalusta case the alteration process seems to have followed the transformation steps given below (Table X). For the sake of simplicity let us consider the face-centred cubic cell as tetragonal as shown in Fig. 12.

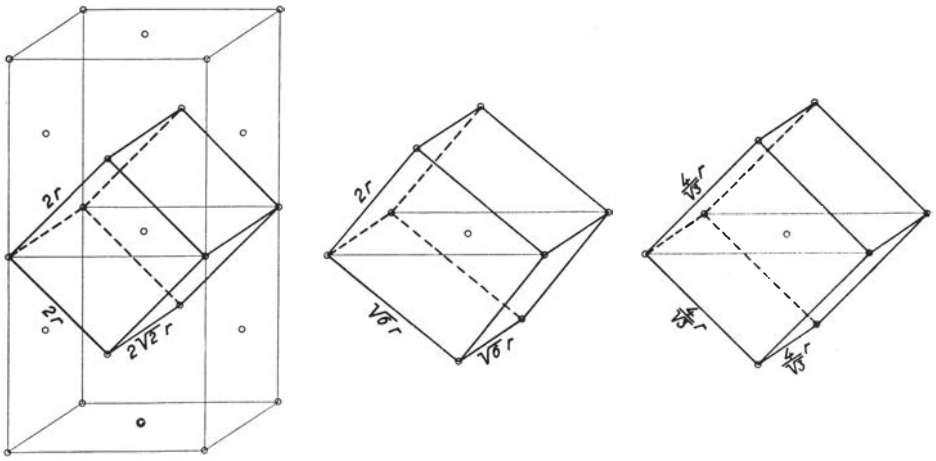

Fig. 12. Transformation steps from the cubic face-centred cell (a) via the tetragonal cell (b) to the cubic body-centred cell (c).

Table X. Transformation steps.

	Direction in the cubic f.-c. cell		Direction in the tetr. cell		Direction in the cubic b.-c. cell
	$[0\,1\,\bar{1}]$	→	$[0\,0\,1]$	→	$[0\,0\,1]$
Edge lengths	$2r$	same length	$2r$	expansion	$2.31\,r$
	$[0\,1\,1]$	→	$[0\,1\,0]$	→	$[0\,1\,0]$
Edge lengths	$2r$	expansion	$2.45\,r$	contraction	$2.31\,r$
	$[1\,0\,0]$	→	$[1\,0\,0]$	→	$[1\,0\,0]$
Edge lengths	$2.84\,r$	contraction	$2.45\,r$	contraction	$2.31\,r$

As is shown in the scheme of Table X and in Fig. 12 *a*, *b*, *c* a transformation mechanism has been chosen via the tetragonal cell in such a manner that if the cubic face-centred lattice is transformed to the closest packed tetragonal cell the displacement of the atoms are relatively smaller than if directly transformed to the cubic body-centred lattice. The transitional step has functioned like a tooth in a gear wheel with the two teeth on either side corresponding to the cubic cells.

The 10-fold co-ordination of the tetragonal cell is anomalous and the symmetry of the bond directions are not so high as in the cubic cells which supports the assumption that the tetragonal cell is metastable. The author does not know of any cell built up in a similar manner among the true metals. Among the B-sub-groups metals (23) however, white tin appear to have an atomic arrangement built up according to principles similar to the tetragonal cell in question. As is known, white tin is a modification of tin, being metastable at

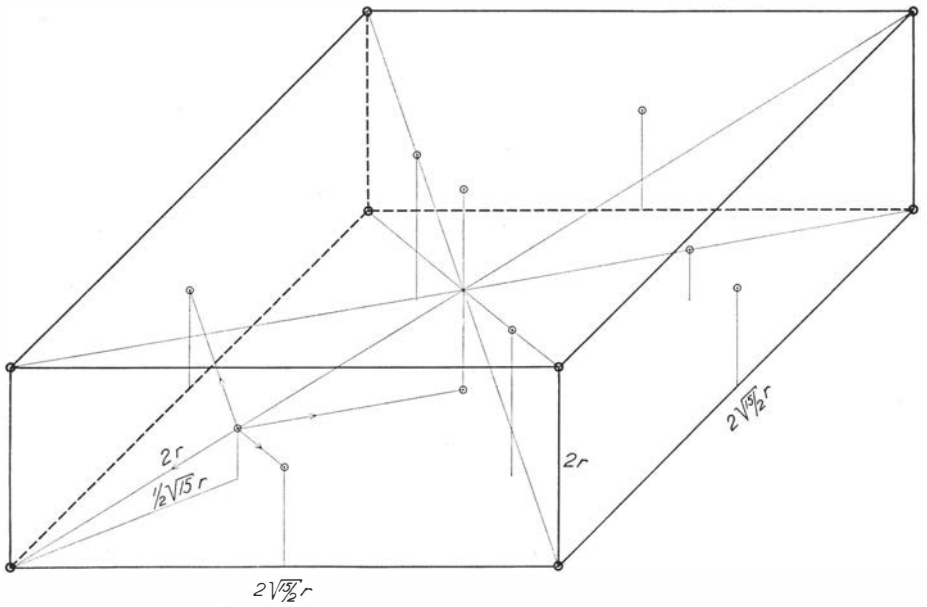

Fig. 13. Unit cell of white tin with approximative edge-lengths.

room temperature and having tetragonal symmetry. By cooling to low temperature white tin is transformed to grey tin with cubic symmetry.

The structure of white tin has been determined by H. MARK and M. POLANYI (24) who found that the tetragonal unit cell contains 8 atoms having the coordinates

$$000,\quad 0\tfrac{1}{2}\tfrac{1}{2},\quad \tfrac{1}{2}0\tfrac{1}{2},\quad \tfrac{1}{2}\tfrac{1}{2}0,$$
$$\tfrac{1}{4}\tfrac{1}{4}\tfrac{1}{4},\quad \tfrac{1}{4}\tfrac{3}{4}\tfrac{3}{4},\quad \tfrac{3}{4}\tfrac{1}{4}\tfrac{3}{4},\quad \tfrac{3}{4}\tfrac{3}{4}\tfrac{1}{4}.$$

The axial ratio $\frac{c}{a}$ was found to be 0.381 or about $\sqrt{\frac{2}{15}} = 0.365$. As is illustrated in Fig. 13 every atom has two neighbouring atoms in the positive and negative directions of the c-axis and four neighbouring atoms situated $\sqrt{\frac{15}{2}}\,r$ to the sides (in the plane of the a- and b-axes) and $\frac{r}{2}$ higher or lower (along the c-axis) than the atom in question. We have in that manner approximately a 6-fold co-ordination instead of normally a 4-fold one. The packing of the tin cell is not so close as in the closest packed tetragonal cell but the anomalous $(4+2)$-fold co-ordination is due to approximately the same structural principles as the anomalous $(8+2)$-fold co-ordination of the closest packed tetragonal cell.

Conclusions.

The result of the above discussion is the conclusion that the most probable explanation of the anomalous orientation of the lamellae of the Muonionalusta structure is dependent on the existence of a tetragonal phase formed during the cooling process of the iron meteorite. It is probably a transitional phase between the γ- and the α-phases of the iron-nickel system. The lattice of the tetragonal phase corresponds to a specific, simple tetragonal lattice of a so-called closest tetragonal packing.

The positive proof of the existence of the tetragonal phase is the specific orientation of lamellae of the iron meteorite. A secure foundation for the hypothesis can futher be established only by verifying experimentally that a tetragonal phase really does exist in the iron-nickel system. Until this has been verified we must as above restrict our discussion to be more or less speculative. The very simple arrangement of atoms in the tetragonal phase according to the hypothesis is at least a negative proof for the correctness of the same. In this respect the hypothesis is in accordance with the postulate of simplicity which, notwithstanding all divergences of detail, seems to be valid in Nature.

The transformation mechanism is probably more complicated in its details than is evident from the schemes above but nevertheless, the hypothesis may contain a nucleus of truth. It is futile to discuss the mechanism in more detail until it can be studied experimentally. Concerning the X-ray analysis it can be predicted that on a DEBYE-SCHERRER diagram the interferences of the tetragonal phase must lie near the interferences from planes having small indices of the α-phase but not so near as those of the α_2-phase which are shown on the spectra published by OWEN and BURNS (10).

The formation of the WIEDMANNSTÄTTEN structure is surely very closely connected to the transformation mechanism of the lattice. But most of the facts concerning this subject are still unknown. It may be pointed out in this connection that the reason why the lamellae of the Muonionalusta iron are orientated parallel to the faces of a tetragonal pyramid (111) also — if we accept the opinion that the orientation is somehow connected with the hypothetical tetragonal lattice — is unclear for these planes do not represent the planes of the closest packing of atoms.

Another question — which has previously been mentioned but which has by no means been solved — is this: Does the tetragonal phase influence the lamellar orientation of iron meteorites in general or only in special cases as in the Muonionalusta case? The result of some random samples (see appendix) seems to indicate that the Muonionalusta structure is more uncommon among the iron meteorites than the octahedral structure. The formation of the tetragonal phase is possibly restricted to iron meteorites of specific chemical compositions although the random samples do not show such a connection clearly.

Finally, it should be emphasized that it would be of interest if the metallurgist, engaged in studying the equilibrium conditions of iron-nickel alloys, would take the viewpoints discussed above into consideration. The experimental verification of the hypothetical tetragonal phase should complete the equilibrium diagram. But besides this a knowledge of the characteristics of the phase is perhaps a necessary qualification for a better understanding of the structure of octahedrites and for carrying out a successful synthesis of them.

Appendix.

In order to compare the structure of some other meteoric irons with the structure of the Muonionalusta iron the author has determined a few sections of other irons according to the method described in Chapter II. The first meteorite determined in this manner is an iron meteorite from Narraburra Creek. The necessary angule determinations were carried out by LEONHARDT (loc. cit. p. 188). The other meteorites investigated belong to the meteorite collection of the Mineralogical Geological Institution in Uppsala. A few of these meteorites have four lamellar systems well developed.

a) Narraburra Creek.

This meteorite belongs to the group of fine octahedrites. It is poor in plessite and its chemical analysis is 88.6 % Fe, 9.7 % Ni and 0.5 % Co.

According to LEONHARDT the angles between the four lamellae were found to be

$$\psi_1 = 14^\circ\ 15'$$
$$\psi_2 = 59^\circ\ 30'$$
$$\psi_3 = 29^\circ\ 0'$$
$$\psi_4 = 77^\circ\ 15'$$

which gives

$$l_1 = 0^\circ \qquad l_2 = 14.2^\circ \qquad l_3 = 73.7^\circ \qquad l_4 = 102.7^\circ.$$

Groups 3, 10, 14 and 20 are excluded. Groups 1, 2, 11, 12, 15, 17, 19, 21 as well as 20 subgroups are then possible. Of these, all groups and 18 subgroups are impossible or are excluded according to limiting condition II. The remaining angle combinations are

	$\alpha_{1,2}$	$\alpha_{1,3}$	$\alpha_{1,4}$	
1)	239.5°	268.5°	345.8°	Group 8, subgroup 3
2)	88.5	165.8	239.5	» 9, » 6.

For the octahedron case the first angle combination gives, when $\varrho = 67.8^\circ$ the smallest differences between the φ-values. For $\alpha_{1,2}$ $\varphi = 79.6^\circ$; for $\alpha_{1,3}$ $\varphi = 80.3^\circ$; for $\alpha_{1,4}$ $\varphi = 82.1^\circ$. The second combination gives, when $\varrho = 23.5^\circ$ the smallest differences. For $\alpha_{1,2}$ $\varphi = 19.0^\circ$; for $\alpha_{1,3}$ $\varphi = 24.7^\circ$; for $\alpha_{1,4}$ $\varphi = 20.9^\circ$.

The coordinates of the two possible sections are thus

1) $\varphi = 81^\circ$ $\varrho = 68^\circ$
2) $\varphi = 22$ $\varrho = 24$

The first solution seems to be the most probable one. The second however, is nearly the same as LEONHARDT's solution who found the possible section to have the indices (1132. 2667. 6942). The coordinates of a section with these indices may be found on calculation to be $\varphi = 21^\circ$, $\varrho = 24^\circ$.

The angle combinations on the section can be brought in accordance with diagram I for the octahedron case only and it appears therefore that the *Narraburra Creek meteorite is a true octahedrite*.

b) Gibeon.

In the meteorite collection there are three examples of iron meteorites which are denoted as Gibeon. The largest of them (M. 19) is a slab whose dimensions are approx. $30 \times 20 \times 1$ cm. On the polished and etched section of this slab four lamellar systems are very well developed.

The meteorite from Gibeon (in the literature it is often denoted as Bethany or Mukerop)[1] is a fine octahedrite relatively rich in plessite and with about 91—94 % Fe, 8 % Ni and 0.5 % Co.

The angles between the lamellar systems were determined to be

$$l_1 \wedge l_2 = 38.7^\circ \pm 0.9^\circ \quad l_2 \wedge l_3 = 30.7^\circ \pm 1.3^\circ \quad l_3 \wedge l_4 = 37.9^\circ \pm 0.8^\circ$$

or

$$l_1 = 0^\circ \quad l_2 = 38.7^\circ \quad l_3 = 69.4^\circ \quad l_4 = 107.3^\circ.$$

Groups 1, 2, 3, 5, 7, 10, 12, 14, 16, 17, 20 and 22 are excluded. Groups 11, 15, 19, 21 as well as 11 subgroups are then possible. Of these, 3 groups and 9 subgroups are excluded according to limiting condition II. The remaining angle combinations are

	$\alpha_{1,2}$	$\alpha_{1,3}$	$\alpha_{1,4}$	
1)	210.7°	248.6°	321.3°	Group 8, subgroup 3
2)	68.6	141.3	210.7	» 9, » 6
3)	290.6	329.3	37.9	» 15.

[1] See L. J. SPENCER, The Gibeon Shower of Meteoric Irons in South-West Africa. The Min. Mag. (1941) *26*, 19.

For the octahedron case the first angle combination gives, when $\varrho = 56.5^\circ$ the smallest differences between the φ-values. For $\alpha_{1,2}$ $\varphi = 91.3^\circ$; for $\alpha_{1,3}$ $\varphi = 91.8^\circ$; for $\alpha_{1,4}$ $\varphi = 90.3^\circ$. The second combination gives when $\varrho = 34.0^\circ$ the smallest differences. For $\alpha_{1,2}$ $\varphi = 1.5^\circ$; for $\alpha_{1,3}$ $\varphi = 0.6^\circ$; for $\alpha_{1,4}$ $\varphi = -1.6^\circ$. The third combination gives for $\varrho = 89.5^\circ$ the smallest differences. For $\alpha_{1,2}$ $\varphi = 56.7^\circ$; for $\alpha_{1,3}$ $\varphi = 56.5^\circ$; for $\alpha_{1,4}$ $\varphi = 56.4^\circ$. The third combination seems to be the most probable one and the coordinates are

$$\varphi = 57^\circ$$
$$\varrho = 90^\circ.$$

The occurrance of three solutions depends on the fact that the section lies very near the zone [001] (see page 297). All three solutions are almost identical from a crystallographic point of view.

The angle combinations on the section can be brought in accordance with diagram I only and *the Gibeon meteorite of this type is as the foregoing a true octahedrite.*

c) Descubridora.

In the meteorite collection there is one slab denoted as Descubridora (M. 14). The dimensions of the slab are approx. $11 \times 9 \times 1$ cm. On the polished and etched section c_d of the slab three lamellar systems l_2, l_3, l_4 are well developed. The lamellae of the lamellar system l_2 is somewhat broader than the other two systems. The lamellae of the fourth lamellar system l_1 have a pronounced width and are more difficult to discern. They seem to lie nearly parallel to the section.

The Descubridora meteorite is a medium octahedrite relatively rich in plessite and with about 89.5—90 % Fe, 8.0 % Ni and 1.9 % Co.

The angles between the lamellar systems were determined to be

$$l_1 \wedge l_2 = 30.3^\circ \pm 1.4^\circ \qquad l_2 \wedge l_3 = 47.3^\circ \pm 0.8^\circ \qquad l_3 \wedge l_4 = 69.0^\circ \pm 0.6^\circ$$

or

$$l_1 = 0^\circ \qquad l_2 = 30.3^\circ \qquad l_3 = 77.6^\circ \qquad l_4 = 146.6^\circ.$$

For the octahedron case groups 3, 6, 8, 10, 12, 13, 14, 21 and 24 are excluded. Groups 1, 11, as well as 21 subgroups are then possible. Of these the two groups and 18 subgroups are impossible or are excluded according to limiting condition II. The remaining angle combinations are

	$\alpha_{1,2}$	$\alpha_{1,3}$	$\alpha_{1,4}$				
1)	210.3°	257.6°	326.6°	Group	1,	subgroup	7
2)	77.6	146.6	210.3	»	4,	»	4
3)	326.6	30.3	257.6	»	5,	»	1.

The first angle combination gives, when $\varrho = 55.6^\circ$ the smallest differences between the φ-values. For $\alpha_{1,2}$ $\varphi = 71.3^\circ$; for $\alpha_{1,3}$ $\varphi = 71.1^\circ$; for $\alpha_{1,4}$ $\varphi = 70.8^\circ$. The second combination gives, when $\varrho = 39.4^\circ$ the smallest differences between the φ-values. For $\alpha_{1,2}$ $\varphi = 26.4^\circ$; for $\alpha_{1,3}$ $\varphi = 26.0^\circ$; for $\alpha_{1,4}$ $\varphi = 25.3^\circ$. The third combination gives in the same manner the smallest differences, when $\varrho = 74.0^\circ$. For $\alpha_{1,2}$ $\varphi = 36.5^\circ$; for $\alpha_{1,3}$ $\varphi = 36.4^\circ$; for $\alpha_{1,4}$ $\varphi = 36.3^\circ$.

The third solution seems to be less probable because according to it we must assume lamella l_2 to lie in the 1st quadrant. It is not possible to judge which of the two other solutions is the right one. Thus the coordinate of the section may be

1) $\varphi = 71^\circ$ $\varrho = 56^\circ$

or

2) $\varphi = 26$ $\varrho = 39$.

For the Muonionalusta case groups 2, 3, 6, 8, 10, 12, 13, 14, 20, 21, 24 are excluded. Groups 1, 11 as well as 19 subgroups are then possible. Of these the two groups and 18 subgroups are impossible or are excluded according to limiting condition II. The remaining angle combination is

$\alpha_{1,2}$	$\alpha_{1,3}$	$\alpha_{1,4}$	
77.6°	146.6°	210.3°	Group 4, subgroup 4.

The angle combination gives, when $\varrho = 31.9^\circ$ the smallest differences between the φ-values. For $\alpha_{1,2}$ $\varphi = 18.5^\circ$; for $\alpha_{1,3}$ $\varphi = 19.6^\circ$; for $\alpha_{1,4}$ $\varphi = 19.1^\circ$. For the Muonionalusta case we thus have a third possible solution with the coordinates

3) $\varphi = 19^\circ$ $\varrho = 32^\circ$.

Consequently it is impossible on this section to decide whether we have a true octahedrite or not. For this reason a section a_d lying nearly perpendicular to c_d was cut, polished and etched. On section a_d three lamellar systems l_1, l_2 and l_3 were dicernible. The following angles were determined

$$\begin{aligned}
&\measuredangle\, c_d \wedge \measuredangle\, a_d = 90.5^\circ \pm 0.2^\circ,\\
&[c_d\, a_d] \wedge [a_d\, l_1]^1 = \ 12.1^\circ \pm 0.3^\circ\\
&[c_d\, a_d] \quad [a_d\, l_3] \ = \ 71.5 \ \pm 0.3\\
&[c_d\, a_d] \quad [a_d\, l_2] \ = 127.9 \ \pm 0.6\\
&[c_d\, a_d] \quad [c_d\, l_3] \ = 118.8 \ \pm 0.1.
\end{aligned}$$

[1] I. e., the angle between edge $[c_d\, a_d]$ and the trace of lamella l_1 on the section a_d measured clock-wise.

From the last value and the above mentioned angle determinations on the section c_d the following angles may be calculated

$$[c_d\, a_d] \wedge [c_d\, l_1] = 41.2^\circ$$
$$[c_d\, a_d] \quad [c_d\, l_2] = 71.5.$$

If we choose a coordinate system in such a manner that the normal to the section c_d lies parallel to [001] and the edge $[c_d\, a_d]$ lies parallel to [010] the coordinates of the poles of lamellae l_1, l_2 and l_3 can be calculated to be

1) Lamella l_1 $\varphi = 311.2^\circ$ $\varrho = 18.1^\circ$
2) Lamella l_2 $\varphi = 161.5$ $\varrho = 53.7$
3) Lamella l_3 $\varphi = 28.8$ $\varrho = 73.5$.

From this the interlamellar angles

$$\perp l_1 \wedge \perp l_2 = 69.7^\circ$$
$$\perp l_2 \wedge \perp l_3 = 110.8 \text{ (supplementary angle } 69.2^\circ)$$
$$\perp l_1 \wedge \perp l_3 = 70.4^\circ$$

can be calculated.

It is thus evident that *the Descubridora iron meteorite is a true octahedrite*.

The coordinates of the middle point of the arc of the great-circle between the poles of lamellae l_2 and l_3 are further $\varphi = 83.9^\circ$, $\varrho = 39.5^\circ$. If we now rotate the system 39.5° around an axis perpendicular to a plane through the last mentioned point and the [001]-axes the point coincides with [001]. On rotating the system a further 124.2° clockwise around [001] the new coordinates are calculated to be

1) Lamella l_1 $\varphi = 44.6^\circ$ $\varrho = 53.1^\circ$
2) Lamella l_2 $\varphi = 315.3$ $\varrho = 55.4$
3) Lamella l_3 $\varphi = 135.3$ $\varrho = 55.4$
4) Pole of sect c_d $\varphi = 28.1$ $\varrho = 39.5$.

As seen the coordinates of the pole of section c_d correspond rather well to the second solution above.

Acknowledgements.

In the preparation of the present paper my friend and former teacher Professor Emeritus HELGE BACKLUND has been of great help to me in numerous ways. For the experimental part of the work he genereously placed the re-

[1] I. e., the polo of lamella l_1.

quisite equipment at my disposal and gave me much valuable guidance for facilitating my work. He subsequently reviewed the manuscript and arranged about its printing. To his successor in the Chair, Professor ERIK NORIN, I am also much indebted for his ready courtesy in providing facilities in the form of literature and meteorite samples necessary for the continuance of the research. I herewith wish to tender to both my profound gratitude for the assistance I received.

The preparation of the necessary samples of the Muonionalusta iron has been carried out by Mr. A. ANDERSSON, former Preparator at the Geological Institution. The English text has been revised and corrected by Mr. CECIL BLACK, Huskvarna. The drawings have been prepared by Mr. EMANUEL STENLUND, Boliden and the manuscript has been typed by my wife, LI MALMQVIST, Boliden. I wish to thank most sincerely those mentioned for their help and contributions towards the completion of the work.

Angle-Table for the »Octahedron»-Case.

φ	ϱ	$\alpha_{1,2}$	$\alpha_{1,4}$	$\alpha_{1,3}$
0°	0°	90.0°	270,0°	180.0°
0	15	86.1	250.5	164.5
0	30	73.9	220.2	146.3
0	45	54.7	180.0	125.3
0	60	33.7	139.8	106.1
0	75	15.5	109.5	94.0
0	90	0.0	90.0	90.0
15	15	90.2	251.7	168.8
15	15.5	90.0	—	—
15	30	80.7	222.8	152.8
15	45	56.9	182.7	126.1
15	46.0	—	180.0	—
15	60	25.1	137.6	95.8
15	63.6	—	—	90.0
15	75	0.1	104.9	76.4
15	75.5	0.0	—	—
15	86.0	—	90.0	—
15	90	344.5	86.0	70.5
30	15	95.1	254.9	174.0
30	30	92.7	234.2	164.1
30	33.6	90.0	—	—
30	45	70.5	197.0	137.6
30	49.1	—	180.0	—
30	56.6	—	—	90.0
30	60	10.3	127.0	77.1
30	63.4	0.0	—	—
30	73.9	—	90.0	—
30	75	338.7	88.3	46.4
30	90	326.3	73.9	40.2
37.5	15	97.8	257.1	177.0
37.5	30	100.7	241.8	171.8
37.5	44.1	90.0	—	—
37.5	45	87.9	214.8	153.1
37.5	51.5	—	180.0	—
37.5	55.1	—	—	90.0
37.5	58.6	0.0	—	—
37.5	60	354.4	109.4	54.7
37.5	66.0	—	90.0	—
37.5	75	322.9	73.7	25.0
37.5	90	316.0	65.0	20.9
45	15	100.4	259.6	180.0
45	30	109.5	250.5	180.0
45	45	116.5	243.5	180.0
45	60	299.9	58.4	0.0
45	75	304.4	55.6	0.0
45	90	305.3	54.7	0.0

φ	ϱ	$\alpha_{1,2}$	$\alpha_{1,4}$	$\alpha_{1,3}$
52.5°	15°	102.9°	262.2°	183.0°
52.5	30	118.2	259.3	188.2
52.5	44.1	—	270.0	—
52.5	45	145.2	272.1	206.9
52.5	51.5	180.0	—	—
52.5	55.1	—	—	270.0
52.5	58.6	—	360.0	—
52.5	60	250.6	5.6	305.3
52.5	66.0	270.0	—	—
52.5	75	286.3	37.1	335.0
52.5	90	295.0	44.0	339.1
60	15	105.1	264.9	186.0
60	30	125.8	267.3	195.9
60	33.6	—	270.0	—
60	45	163.0	289.5	222.4
60	49.1	180.0	—	—
60	56.6	—	—	270.0
60	60	233.0	349.7	282.9
60	63.4	—	360.0	—
60	73.9	270.0	—	—
60	75	271.7	21.3	313.6
60	90	286.1	33.7	319.8
75	15	108.3	269.8	191.2
75	15.5	—	270.0	—
75	30	137.2	279.3	207.2
75	45	177.3	303.1	233.9
75	46.0	180.0	—	—
75	60	222.4	334.9	264.2
75	63.6	—	—	270.0
75	75	255.1	359.9	283.6
75	75.5	—	360.0	—
75	86.0	270.0	—	—
75	90	274.0	15.5	289.5
90	15	109.5	273.9	195.5
90	30	139.8	286.1	213.7
90	45	180.0	305.3	234.7
90	60	220.2	326.3	253.9
90	75	250.5	344.5	266.0
90	90	270.0	360.0	270.0

Angle-Table for the »Muonionalusta»-Case.

φ	ϱ	$\alpha_{1,2}$	$\alpha_{1,4}$	$\alpha_{1,3}$
0°	0°	90.0°	270.0°	180.0°
0	15	85.0	246.0	160.9
0	30	70.1	208.4	139.6
0	39.3	—	180.0	—
0	45	48.4	161.9	113.5
0	60	28.1	121.5	93.4
0	63.5	—	—	90.0
0	75	12.5	94.5	82.0
0	78.5	—	90.0	—
0	90	0.0	78.5	78.5
15	15	90.0	247.4	166.0
15	30	77.4	212.3	145.2
15	40.2	—	180.0	—
15	45	48.1	163.5	112.2
15	54.7	—	—	90.0
15	60	16.9	117.6	80.5
15	72.6	0.0	—	—
15	75	357.1	90.0	64.5
15	90	345.0	75.0	60.0
30	15	96.1	251.5	172.7
30	30	91.6	225.1	159.0
30	31.5	90.0	—	—
30	43.3	—	180.0	—
30	45	54.7	171.6	116.5
30	50.5	—	—	90.0
30	58.5	0	—	—
30	60	357.3	101.4	55.9
30	64.7	—	90.0	—
30	75	336.9	75.3	37.2
30	90	328.5	64.8	33.3
37.5	15	99.4	254.3	176.2
37.5	30	106.8	235.0	164.9
37.5	40.3	90.0	—	—
37.5	45	69.6	186.6	129.7
37.5	45.6	—	180.0	—
37.5	49.5	—	—	90.0
37.5	57.5	—	90.0	—
37.5	53.2	0	—	—
37.5	60	336.7	82.5	33.1
37.5	75	324.0	62.2	19.5
37.5	90	319.7	57.4	17.2
45	15	102.6	257.4	180.0
45	30	113.4	246.6	180.0
45	45	120.9	239.1	180.0
45	60	306.9	53.1	0.0
45	75	309.9	50.1	0.0
45	90	310.9	49.1	0.0

φ	ϱ	$\alpha_{1,2}$	$\alpha_{1,4}$	$\alpha_{1,3}$
52.5°	15°	105.7°	260.6°	183.8°
52.5	30	125.0	258.2	195.1
52.5	40.3	—	270.0	—
52 5	45	173.4	290.4	230.3
52.5	45.6	180	—	—
52.5	53.2	—	360.0	—
52.5	49.5	—	—	270.0
52.5	57.5	270	—	—
52.5	60	277.5	23.3	326.9
52.5	75	297.8	36.0	340.5
52.5	90	302.6	40.3	342.8
60	15	108.5	263.9	187.3
60	30	134.9	268.4	201.0
60	31.5	—	270.0	—
60	43.3	180.0	—	—
60	45	188.4	305.3	243.5
60	50.5	—	—	270.0
60	58.5	—	360.0	—
60	60	258.6	2.7	304.1
60	64.7	270.0	—	—
60	75	284.7	23.1	322.8
60	90	295.2	31.5	326.7
75	15	112.6	270.0	194.0
75	30	147.7	282.6	214.8
75	40.2	180.0	—	—
75	45	196.5	311.9	247.8
75	54.7	—	—	270.0
75	60	242.4	343.1	279.5
75	72.6	—	360.0	—
75	75	270.0	2.9	295.5
75	90	285.0	15.0	300.0
90	15	114.0	275.0	199.1
90	30	151.6	288.7	220.4
90	39.3	180.0	—	—
90	45	198.1	311.6	246.5
90	60	238.5	331.9	266.6
90	63.5	—	—	270.0
90	75	265.5	347.5	278.0
90	78.5	270.0	—	—
90	90	281.5	360.0	281.5

References.

1. N. ZENZÉN: Demonstration of the New Meteorite at the Geological Society in Stockholm. G. F. F. (1946) *68*, 501.
2. A. G. HÖGBOM: Über einen Eisenmeteorit von Muonionalusta im nördlichsten Schweden. Bull. of the Geol. Inst. of Upsala (1910) IX, 229.
3. A. HIMMELBAUER: Orientierung von Schnittflächen an Meteoreisen. Tschermaks Min. und Petrogr. Mitteilungen (1909) *28*, 153.
4. J. LEONHARDT: Die morphologischen und strukturellen Verhältnisse der Meteoreisen im Zusammenhang mit ihrem Entwicklungsgang. N. Jahrb. f. Min. etc. (1928) B. Bd., Abt. A. *58*, 153.
5. F. BERWERTH: Ein natürliches System der Eisenmeteoriten. Sitzungsber. der Kaiserl. Akad. der Wissensch. (1914) Abt. I, *23*, 1047.
6. F. RINNE and H. E. BOEKE: El Inca, ein neues Meteoreisen. N. Jahrb. f. Min. etc. (1907). Festbd. p. 236.
7. E. PFANN: Über den inneren Gefügebau der meteorischen Nickeleisen. Intern. Zeitschr. f. Metallographie (1918) *9*, 65.
8. E. R. JETTE and F. FOOTE: X-Ray Study of Iron-Nickel Alloys. Trans. A. I. M. E. (1936) *120*, 259.
9. W. FRAENKEL and G. TAMMANN: Über meteorisches Eisen. Zeitschr. f. anorg. Chemie (1908) *60*, 432.
10. E. A. OWEN and B. D. BURNS: X-Ray Study of some Meteoric Irons. Phil. Mag. (1939) *28* (7), 497.
11. C. BENEDICKS: One-Phase or Two-Phase Conditions in the System Fe-Ni; Theories of Meteoric Iron and Invar. Arkiv f. Mat., Astron., Fysik (1942) *28 A* (*14*), 13.
12. C. BENEDICKS: Synthèse du fer météorique. Nova Act. Reg. Soc. Sci. Upsaliensis (1910) *IV* (*2*). Nr. 10.
13. F. OSMUND and G. CARTAUD: Sur les fers météorique. Compt. Rend. (1903) 137, 1057.
14. D. HANSON and H. E. HANSON: The Constitution of Nickel-Iron Alloys. Journ. Iron and Steel Inst. (1920) *II*, 39.
15. D. HANSON and J. R. FREEMAN: The Constitution of the Alloys of Iron and Nickel. Journ. Iron and Steel Inst. (1923) *I*, 301.
16. A. J. BRADLEY and H. J. GOLDSCHMIDT: An X-Ray Investigation of the Iron-Rich Nickel-Iron Alloys. Journ. Iron and Steel Inst. (1939) *II*, 11.
17. E. A. OWEN and A. H. SULLY: The Equilibrium Diagram of Iron-Nickel Alloys. Phil. Mag. (1939) *27* (*1*), 614.
18. F. RINNE: Physikalisch-chemische Bemerkungen über technisches und meteorisches Eisen. N. Jahrb. f. Min. (1905) *I*, 150.
19. C. H. JOHANSSON and J. O. LINDE: Röntgenographische Bestimmungen der Atomanordnung in den Mischkristallreihen Au—Cu und Pd—Cu. Annalen d. Physik (1925) *78*, 439.
20. P. LEECH and C. SYKES: The Evidence for a Superlattice in the Nickel-Iron Alloy Ni_3Fe. (1939) *27* (*1*), 742.
21. G. V. SMITH and R. F. MEHL: Lattice Relationships in Decomposition of Austenite to Pearlite, Bainite and Martensite. A. I. M. E. Metals Techn. (1942) *9*, Techn. Publ. Nr. 1459.
22. P. NIGGLI: Lehrbuch der Mineralogie und Kristallchemie (Berlin 1941), 3rd Edition, Part I p. 640.
23. R. C. EVANS: An Introduction to Crystal Chemistry (Cambridge 1939), p. 96.
24. Ref. Handbuch der Metallphysik (Berlin 1935), Vol. I (1), p. 58.

Description of the micrographs in the Plate.

Fig. 1. Kamacite lamella (upper part of the Figure) with taenite and plessite on either side of the lamella. The plessite matrix shows to some extent a micro-octahedrite structure. Tendency to a "cone"-structure. Face c_1. Magn. approx. 60 ×.

Fig. 2. Kamacite lamella bordered on one side by taenite and plessite and on the other only by a taenite ribbon. Face e_1. Magn. approx. 60 ×.

Fig. 3. Kamacite and plessite with taenite ribbons. The taenite shows a "cone"-structure at the boundary between kamacite and taenite. Face c_1. Magn. approx. 60 ×.

Fig. 4. A small plessite field with eutectoid plessite and micro-octahedrite plessite. Magn. approx. 60 ×.

Fig. 5. Eutectoid plessite and plessite with taenite lamellae in parallel arrangement. Magn. approx. 30 ×.

Fig. 6. Eutectoid plessite at high magnification. The lower part of the plessite field of Fig. 4 magnificated. Magn. approx. 300 ×.

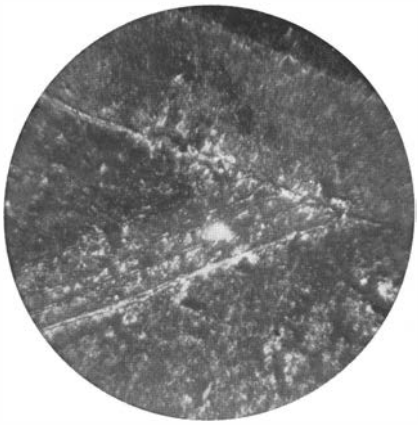

Fig. 1

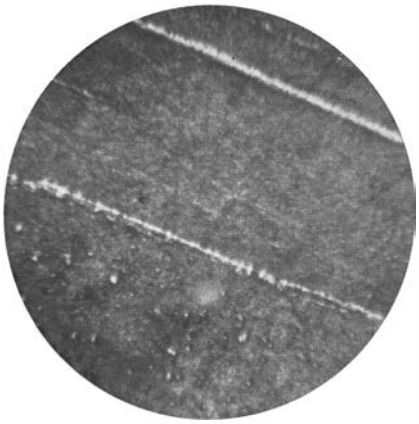

Fig. 2

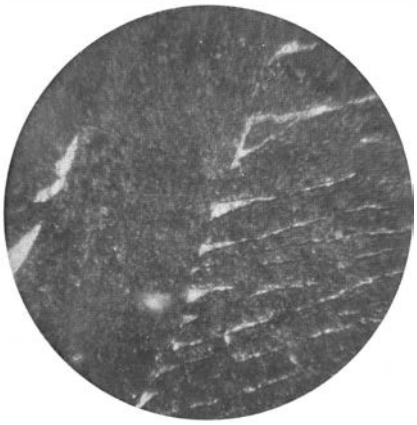

Fig. 3

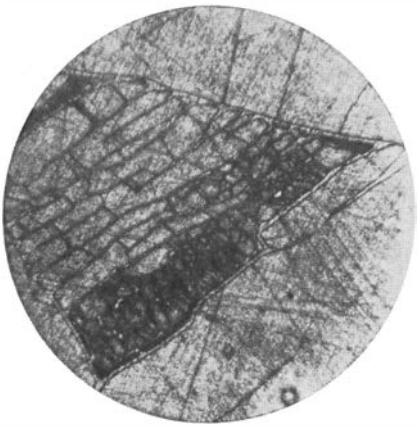

Fig. 4

Fig. 5

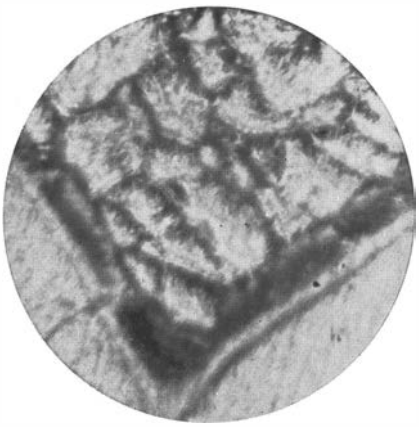

Fig. 6

DIAGRAM 1
THE "OCTAHEDRON" - CASE

Angles between Lamellae on Different Sections

$\alpha_{1,2}$

$\alpha_{1,3}$

$\alpha_{1,4}$

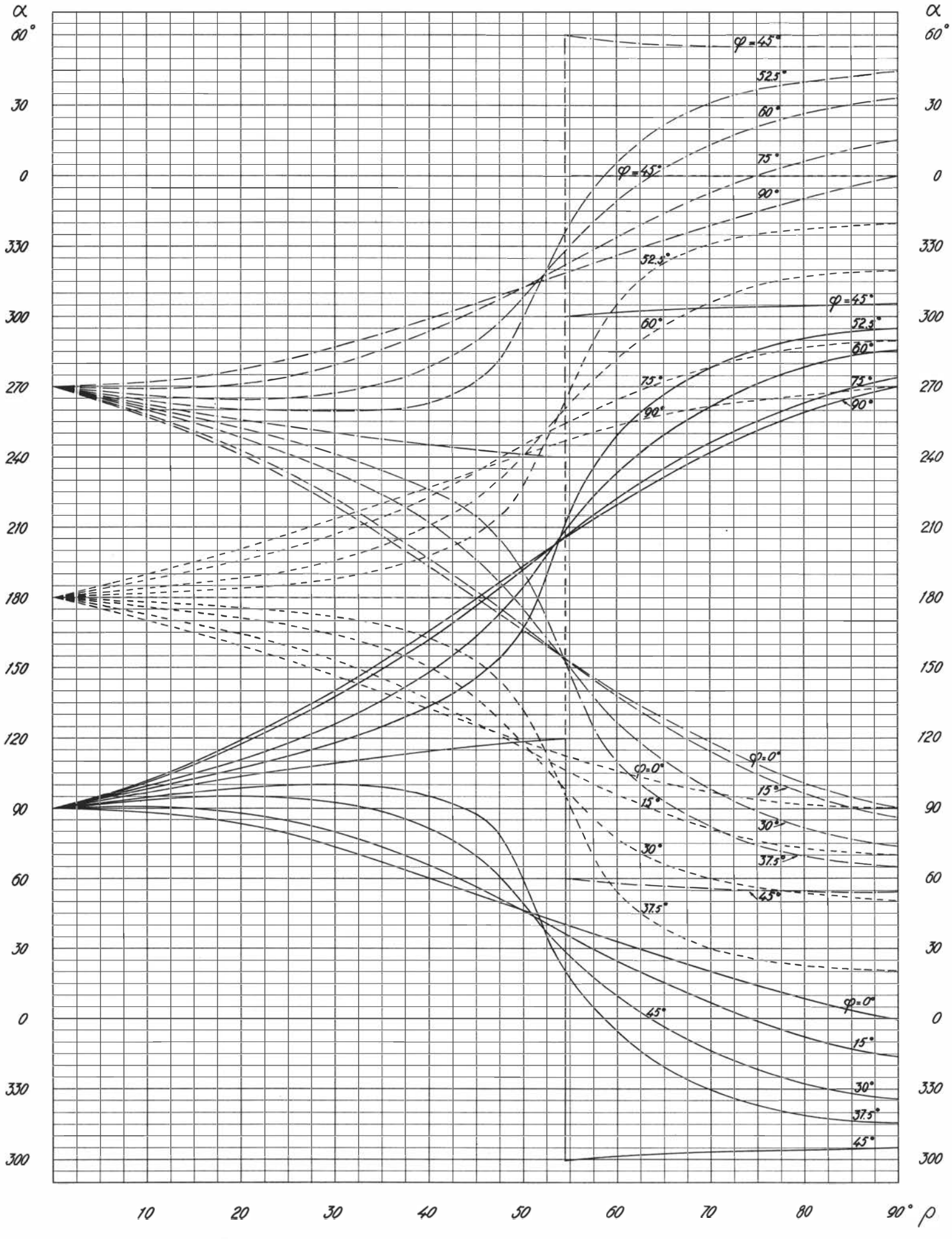

DIAGRAM 2

THE "MUONIONALUSTA" - CASE

Angles between Lamellae on Different Sections

$\alpha_{1,2}$ — △ Section H

$\alpha_{1,3}$ — ⊙ The c_1-Face of Sample 1

$\alpha_{1,4}$ — × " e_2 " " " 2